ADA114404

Velocity Control and Electromechanical Feedback in Sonar Projector Arrays

Ralph S. Woollett
Submarine Sonar Department

Naval Underwater Systems Center
Newport, Rhode Island / New London, Connecticut

DTIC
SELECTE
MAY 1 3 1982

A

82 05 13 094

Preface

This study was conducted under NUSC Project No. A62001, *Advanced Communications Program*, Principal Investigator C. H. Sherman (Code 3292), and Navy Subproject SO918-CC, Program Manager Lloyd Epperly (Code NAVSEA 63D7).

The Technical Reviewer for this report was L. C. Ng (Code 3213).

Reviewed and Approved: 26 April 1982

F. J. Kingsbury

FOR J. W. Kyle
Submarine Sonar Department

The author of this report is located
at the New London Laboratory of the
Naval Underwater Systems Center, New London, CT 06320

REPORT DOCUMENTATION PAGE		READ INSTRUCTIONS BEFORE COMPLETING FORM
1. REPORT NUMBER TR 6629	2. GOVT ACCESSION NO. AD-A114 404	3. RECIPIENT'S CATALOG NUMBER
4. TITLE (and Subtitle) VELOCITY CONTROL AND ELECTROMECHANICAL FEEDBACK IN SONAR PROJECTOR ARRAYS		5. TYPE OF REPORT & PERIOD COVERED
		6. PERFORMING ORG. REPORT NUMBER
7. AUTHOR(s) Ralph S. Woollett		8. CONTRACT OR GRANT NUMBER(s)
9. PERFORMING ORGANIZATION NAME AND ADDRESS Naval Underwater Systems Center New London Laboratory New London, Connecticut 06320		10. PROGRAM ELEMENT, PROJECT, TASK AREA & WORK UNIT NUMBERS
11. CONTROLLING OFFICE NAME AND ADDRESS		12. REPORT DATE 26 April 1982
		13. NUMBER OF PAGES 40
14. MONITORING AGENCY NAME & ADDRESS(If different from Controlling Office)		15. SECURITY CLASS. (of this report) UNCLASSIFIED
		15a. DECLASSIFICATION/DOWNGRADING SCHEDULE

16. DISTRIBUTION STATEMENT (of this Report)

Approved for public release; distribution unlimited.

17. DISTRIBUTION STATEMENT (of the abstract entered in Block 20, if different from Report)

18. SUPPLEMENTARY NOTES

19. KEY WORDS (Continue on reverse side if necessary and identify by block number)

Sonar projector	Motional feedback
Electromechanical transducer	Velocity control
Sonar array	Array interactions
Electromechanical feedback	

20. ABSTRACT (Continue on reverse side if necessary and identify by block number)

Electromechanical feedback has had very little use in sonar-projector arrays because of the complexity it adds to the system. However, its employment may become necessary if a high degree of velocity control is demanded, as might be the case in arrays designed for radiation patterns with very low side lobes.

In this report, the benefits and problems of electromechanical feedback are examined in an introductory manner, largely by numerical examples. The

(over)

DD FORM 1473 EDITION OF 1 NOV 65 IS OBSOLETE
1 JAN 73
S/N 0102-014-6601

20. (Cont'd)

projector in the array mathematical model is assumed to be a simple piezo-
electric type with a single degree of freedom mechanically.

A proposed positive-feedback scheme for neutralizing the effects of
radiation impedance variations was found to operate with too small a margin
of stability to be considered practical. The standard negative-feedback
scheme, using a velocity pickup on the projector, appears promising and
worthy of detailed development. Although the complexity of the negative-
feedback system can be reduced by deriving the feedback signal from the
motional current rather than from the velocity, the practicality of such
a system is dubious. The motional-current signal is obtained by use of an
auxiliary circuit that cancels the current drawn by the blocked capacitance
of the transducer, but the blocked capacitance varies too much with voltage,
temperature, and pressure for this technique to work well.

Before negative electromechanical feedback can be established as a
reliable technique, more extensive stability studies must be carried out.
The present work has shown that the system will not tolerate negative
radiation resistances. In spite of these caveats, negative feedback is
considered a promising approach to better performance whenever the simpler
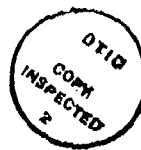Carson method of velocity control is found to be inadequate.

TR 6629

TABLE OF CONTENTS

Page

LIST OF ILLUSTRATIONS

LIST OF ILLUSTRATIONS (Cont'd)

VELOCITY CONTROL AND ELECTROMECHANICAL FEEDBACK
IN SONAR PROJECTOR ARRAYS

INTRODUCTION

In operating a projector array, it is desirable to be able to prescribe the value of the velocity (in magnitude and phase) of every transducer in the array. Only in this way can one realize the shading functions and steering phase distributions that are deemed necessary for optimum radiation patterns, since the patterns are determined by the velocities.

Unfortunately, the input and output ports of a transducer are loosely coupled, and the outputs are influenced by interelement coupling. Thus, if one imposes the desired shading and phasing distribution on the voltages applied to the transducers in the array, there is vanishing probability that the distribution of velocities will replicate the distribution of voltages. The situation is no better if the reference variable is the transducer current, rather than the voltage. The tendency of the output distributions to diverge from the input distributions is brought about by the acoustic coupling in the array, which causes different transducers to have different radiation impedances. The differing radiation impedances, in turn, cause the transducers to have different transmission losses.

One can, of course, calculate the voltages that should be applied to the projectors to obtain the set of velocities that is desired. This approach to array excitation generally is not favored because of uncertainties in the mathematical models and because the transducer parameters may change due to aging. Looking for other solutions to the problem is facilitated if we enlarge the system under study by adding an amplifier and tuning network to each projector in the array. Then, the amplifier inputs are taken as the reference signals. If the transducer velocities can be made to have the same amplitude and phase distributions as the reference input signals, we say we have velocity control. The transducer velocity is, then, the controlled variable in the servomechanism sense. Having the velocities under direct control not only facilitates pattern synthesis but, also, ensures that no transducer will inadvertently be driven beyond its stress limit.

Carson showed that velocity control can be achieved over a limited bandwidth by optimal adjustment of the tuning network and driving amplifier.[1] He accomplished this without adding to the components that are traditionally present in the driving system. An approach that opens up a wider range of possibilities is the use of electromechanical feedback. By feeding back to the amplifier input a voltage proportional to velocity, the velocity becomes controlled by the reference signal (provided that instabilities can be avoided).

Of course, by opting for velocity control, we give up voltage control. The transducer voltages must vary widely in order to force the velocities to match the reference signals in the presence of widely varying radiation

1

impedances. It is necessary to review the calculated voltage distributions to see that no transducer exceeds its maximum voltage rating. If the maximum voltage rating is exceeded, the array power for the set of excitation signals in use must be reduced until all transducers are under the voltage ceiling. Another drawback of velocity control is that it distorts the frequency response of the system. Pre-equalization probably would be required to keep the response shape in the desired form.

In this report, use of electromechanical feedback will be examined in an introductory manner. The projectors in the array are assumed to be of the piezoelectric type. Both positive and negative feedback will be examined. Stability will be looked at in a preliminary way, but much more work in this area is required before feedback can establish itself as a reliable technique in sonar-array design.

ELECTROMECHANICAL FEEDBACK

Not much time elapsed between the invention of the negative-feedback amplifier and the application of negative feedback to electroacoustical apparatus. The first notable paper was on a high-fidelity record cutter.[2] Applications to loudspeakers soon followed.[3-6] In industrial ultrasonics, feedback was used both for velocity control and frequency control.[7] In sonar, electromechanical feedback was often discussed but did not get into large-scale use. Only a few uses in experimental equipment have been recorded, for example, in a hydroacoustic projector[8] and in a Helmholtz resonator projector.[9]

Electromechanical feedback in large sonar arrays has seemed unattractive because of the complexity of the added feedback channels. The need for such a system has been mitigated by use of projectors with large radiating heads, which minimize interaction effects. With reasonably lenient side-lobe specifications, precise shading has not been required. Thus, even though the velocity distribution did not replicate accurately the reference input distribution, the beam patterns were satisfactory and improved velocity control was not demanded. The stress problem of transducers at high-velocity points in the array also proved manageable if the transducers were conservatively designed. These older arrays appeared to achieve a good compromise between velocity control and voltage control.

As the requirements on sonar-array performance become more rigorous, consideration of the use of electromechanical feedback will be warranted in spite of the added complexity. To prepare for this eventuality, we have undertaken a survey of the benefits and problems that can be expected of feedback techniques; the results are presented here.

The studies to be done here will be based on use of a power amplifier of the constant-voltage type (zero output impedance). Similar studies could be done for a system using a current amplifier and the results would probably not differ greatly. To obtain a signal proportional to velocity, the most straightforward approach is to mount an accelerometer on the projector's radiating member (probably on the inside surface). The output of the accelerometer is integrated electronically with respect to time to provide the velocity

signal. A cable is needed to bring this signal back to the amplifier; so the total number of cables to the transducer is doubled. A severe crosstalk problem may exist, since the feedback signal is very small compared to the driving signal on the neighboring power cable.

The cable problems can be avoided if we derive the feedback signal from the motional current of the transducer rather than from its velocity. The former is constrained to be proportional to the latter by the relationship

$$I_{mot} = NV , \tag{1}$$

where N is the electromechanical transfer ratio, which is a constant. Unfortunately, I_{mot} is not accessible for measurement so an attempt is made to obtain a close approximation to it by use of a compensation circuit. One such circuit arrangement is included in figure 1,* which depicts the entire transmission system for one projector.

In figure 1, I is the transducer input current, which is accessible. This current differs from the motional current, I_{mot}, by the current that flows into the blocked admittance branch, Y_b, of the transducer circuit. We wish to make the subtraction

$$I_{mot} \approx I - Y_b E . \tag{2}$$

For this purpose, we construct a Y_b-simulator circuit with parameter values G_b', C_b' as close to G_b, C_b as possible. This accessible circuit, when connected across the driving cable at the amplifier output, draws approximately the same current as the Y_b branch of the transducer circuit; so we use the simulator current in place of $Y_b E$ in Eq. (2).

The feedback signal in figure 1 is produced by a current transformer that links both the input current, I, and the simulator current, $Y_b' E$. These two currents have opposite directions going through the current transformer; so the desired subtraction takes place. If the simulation is exact ($Y_b' = Y_b$), the feedback signal will be proportional to I_{mot} (which is proportional to V).[10]

A practical modification that would be made in using this arrangement would be to make the wire going to the simulator pass through the current transformer more than once, say 10 times. In such case, $C_b' \approx 0.1C_b$, $G_b' \approx 0.1G_b$, and the reactive power drawn by the simulator from the amplifier would be reduced to an insignificant amount.

The subtraction indicated in Eq. (2) can be made in ways other than by use of current transformers. For instance, a bridge circuit[7] may be used or a differential amplifier may be used. In the case of positive feedback (to be discussed below), the Y_b-simulator circuit of figure 1 is omitted and similar elements are put in the feedback circuit, represented by the β box.

---

*Figures have been grouped together at the end of this report.

Unfortunately, all feedback schemes based on I_{mot} suffer a major disadvantage, which is the variability of C_b. The capacitance of piezoelectric ceramics depends on temperature, stress, and the level of the electric driving field. The loss conductance, G_b, also depends on these variables and, in addition, is inversely proportional to frequency; however, its impact on the feedback effectiveness is less than that of C_b. There appears to be little hope of maintaining the balance between Y_b and Y_b' to closer than 10 percent in high-power variable-depth projectors. Making the simulator out of the same ceramic as that used in the transducer would allow the electric-field dependence to be matched, but subjecting the inboard simulator to the same pressure and temperature as occurs in the transducer would hardly be practical.

MATHEMATICAL MODEL

To show the effect of electromechanical feedback on performance, calculations will be made for the transmission system shown in figure 1. The transducer portion of this system is represented as having a single degree of freedom mechanically; it is valid only for the fundamental mode. However, higher modes are important in determining the stability of the feedback system; they should be included in the models used for later, more definitive, stability studies. Also omitted here, but required for these later studies, are circuits for rolling off the loop gain at low and high frequencies. Negative feedback is indicated at the summing point in figure 1. The equations are, thus, cast in familiar form but positive feedback is achievable by changing the sign of β. Although no tuning inductor is shown in figure 1, a parallel inductor for power-factor correction can be inserted ahead of the current-sampling point without affecting any of the equations that will be presented in the subsequent development.

Calculations will be made over a wide frequency range of the closed-loop system response and of the feedback-loop response. While the frequency is being varied, the radiation components M_{rad} and R_{rad} will be maintained constant at some chosen representative values for an array element. This is not a true operating condition for a projector element in a real array.[11] When the driving frequency of the real array is varied, the radiation impedance of the projector under examination will not follow the smooth curves corresponding to constant M_{rad} and R_{rad}. The reason for the present approach is that it is enormously simpler than doing complete array calculations every time the frequency is changed. The justification for this approach is that it enables us to explore all the regions of Z_{rad}-space that the real array traverses, if we do runs for enough values of M_{rad} and R_{rad}.

The input admittance of the transducer is the sum of a blocked and a motional part,

$$Y_{in} = Y_b + Y_{mot} \cdot \qquad (3)$$

The motional admittance is the reciprocal of an electrical impedance, Z_Y, which is the electrical equivalent of the total mechanical impedance, $Z_M + Z_{rad}$,

$$\frac{1}{Y_{mot}} = Z_Y = \frac{Z_M + Z_{rad}}{N^2} = R_Y + j\omega L_Y + \frac{1}{j\omega C_Y} . \tag{4}$$

The closed-loop response of the system is

$$\frac{I_{mot}}{E} = \frac{AY_{mot}}{1 + A\beta Y_{in}''} = \frac{AY_{mot}}{1 + J(\omega)} , \tag{5}$$

where A is the amplifier gain, β is the feedback transfer function, and

$$Y_{in}'' = Y_{in} - Y_b' . \tag{6}$$

When the Y_b-simulator is perfect, $Y_{in}'' = Y_{mot}$; when the Y_b-simulator is absent, $Y_{in}'' = Y_{in}$ is simply the input admittance of the transducer. Since we wish to control the variable $V = I_{mot}/N$ (by assignment of values to E), Eq. (5) is an appropriate transfer function to study. The power output of the projector is $1/2|V|^2 R_{rad}$ and, since in this study R_{rad} is assumed to be independent of frequency, a plot of Eq. (5) will give the shape of the power frequency response.

The quantity $J(\omega) = A\beta Y_{in}''$ is the feedback factor, or loop gain. In principle, stability is determined by substituting the complex frequency s for ω in this expression and finding whether any of the pole frequencies, s_p, determined by $J(s_p) = -1$ have positive real parts. We will follow the simpler well-established techniques of plotting $J(\omega)$ as a function of ω in the form of a Bode diagram or in the form of a Nyquist diagram.

The closed-loop response of Eq. (5) can be put in an alternate form that brings the velocity control objective into focus,[12]

$$\frac{I_{mot}}{E} = \frac{1/\beta}{1 + Z_Y(Y_b'' + 1/A\beta)} , \tag{7}$$

where

$$Y_b'' = Y_b - Y_b' . \tag{8}$$

The radiation impedance variations are contained in Z_Y and are the source of the array problems. If we can make the expression in parentheses multiplying Z_Y become zero, we will have perfect velocity control. The motional current (or velocity), then, will be determined only by the reference signal, E.

There are two ways to make the multiplier of Z_Y in Eq. (7) become zero, or at least small. In the positive-feedback scheme, for which $Y_b' = 0$ and $Y_b'' = Y_b$, the sum of the terms in the parentheses is made zero. In the negative-feedback scheme, each term in the parentheses, individually, is made as small as possible. These topics will be covered in more detail in later sections.

In the following sections, the various velocity-control techniques will be illustrated with numerical examples. The transducer in all examples is assumed to have an electromechanical coupling factor, k, of 0.4 and a mechanical Q, when operating alone (in the array baffle), of 3. The resonance frequency of the transducer operating alone is designated $f_0 = \omega_0/2\pi$. The radiation impedance of the transducer operating alone is $Z_{self} = R_{self} + j\omega M_{self}$.

The examples will be calculated for a number of representative values of the array radiation impedance, Z_{rad}. Specifying the array loading is facilitated if we define the transducer's resonance frequency and mechanical Q under array loading conditions. The respective equations are

$$\omega_r = \sqrt{\frac{1}{C_M(M + M_{rad})}} = \omega_0 \sqrt{\frac{M + M_{self}}{M + M_{rad}}} \qquad (9)$$

$$Q_M = \frac{1}{\omega_r C_M(R_M + R_{rad})} = 3\frac{\omega_0(R_M + R_{self})}{\omega_r(R_M + R_{rad})} . \qquad (10)$$

Thus, ω_r can be used to reflect the changes in M_{rad}, and Q_M can be used to reflect the changes in R_{rad}.

The array is considered to be formed of large radiators (projector face dimensions of about 0.4 wavelengths) and to include steering angles far off the normal. The resonance frequencies of the projectors in such an array are believed to remain within about 20 percent of the resonance of the projector operating alone. The mechanical Q's of the projectors in the array can go as high as the Q in air (complete unloading) or even can go negative (reflecting negative R_{rad}). The mechanical Q can range as low as 0.3 for the heavily loaded projectors. In the examples here, the values $\omega_r/\omega_0 = 1.2$ and $Q_M = 5$ generally have been used for the initial calculations.

POSITIVE FEEDBACK

Design Automation, Inc., has proposed[12] a velocity control method based on positive feedback. Cancellation of the effect of Y_b takes place in the feedback loop; therefore the simulator in figure 1 is not used. From Eq. (7), the closed-loop response is

$$\frac{I_{mot}}{E} = \frac{1/\beta}{1 + Z_Y(Y_b + 1/A\beta)} . \qquad (11)$$

For perfect velocity control, the feedback is adjusted such that $1/A\beta = -Y_b$. Note that the aim is not to have as much feedback as possible (as with negative feedback) but, rather, to have the precise amount needed for cancellation of Y_b. Under this ideal condition, the response, Eq. (11), reduces to $1/\beta = -AY_b$ and is independent of the radiation impedance, which is contained in Z_Y.

In practice, the cancellation of Y_b will be imperfect, so we specify the residual admittance remaining in terms of real and imaginary parts, a and b, as follows:

$$Y_b + \frac{1}{A\beta} = \omega C_b (a + jb) . \tag{12}$$

Then,

$$\frac{1}{A\beta} = \omega C_b [-\tan \delta + a - j(1 - b)] , \tag{13}$$

where $\tan \delta = G_b/\omega C_b$ is the blocked dissipation factor of the transducer. The feedback factor is

$$J(\omega) = A\beta Y_{in} = \frac{\tan \delta + j + \dfrac{(\omega_1 / \cdots (k^2/(1 - k^2))}{(1/Q_M) + j(\omega/\omega_r - \omega_r/\omega)}}{-\tan \delta + a - j(1 - b)} . \tag{14}$$

In this equation, the electromechanical coupling factor $k = \sqrt{C_Y/(C_b + C_Y)}$ has been introduced. At both low and high frequencies, $J(\omega)$ becomes constant:

$$J(\omega \rightarrow 0) = \frac{\tan \delta + j(1 + k^2/(1 - k^2))}{-\tan \delta + a - j(1 - b)}$$

$$J(\omega \rightarrow \infty) = \frac{\tan \delta + j}{-\tan \delta + a - j(1 - b)} . \tag{15}$$

Near ideal operation of this system is illustrated in figure 2, which is a plot of the closed-loop response relative to a perfect system. In this example, it was assumed that cancellation of the blocked capacitance was accomplished very well, leaving only a 1 percent residual. The magnitude curve shows that, over the operating band, velocity control is perfect within 0.3 dB. The transfer phase is controlled to better than 1 deg. The response of the perfect system, AY_b, has a 6 dB/octave slope. Hence, the slope of the magnitude curve in figure 2 would be increased by this amount if it were an unnormalized plot of Eq. (5).

The stability of the system can be examined by use of the Bode diagram shown in figure 3. This is a plot of the magnitude and phase of the feedback factor, $J(\omega)$, from Eq. (14). Except near resonance, the phase angle runs very close to 180 deg; the phase margin against instability is only a fraction of a degree. The magnitude curve crosses the zero-dB line at 5.3 ω/ω_0 and the close approach to instability at this point is manifest in the 17-dB peak in the closed-loop response, seen in figure 2. Obviously, the phase margin of this system is much too small to be practical.

The cancellation of the blocked admittance assumed for figure 2 was too good to be realistic. In the next example, it is assumed that the blocked capacitance is cancelled to within only 10 percent of its initial value. This is probably as good as can be achieved in practice unless elaborate feedback networks with varying-parameter elements are used. The closed-loop response

for this example is given in figure 4. The magnitude curve shows that the velocity control has deteriorated considerably from that exhibited in figure 2. At the low end of the passband, the velocity has departed 3 dB from the reference value. The transfer phase departs from the reference value by 8 deg at the top of the passband.

The Bode diagram for this example is shown in figure 5. As in the previous case, the phase margin is only a fraction of a degree except in the resonance region. Hence, the system can hardly be considered practical. Since the Bode diagram shows the system to be on the verge of instability, it would be wise to examine this aspect further. For this purpose, the Nyquist diagram (which is a polar plot of the feedback factor $J(\omega)$) was constructed, as shown in figure 6. The frequency ranges from $-\infty$ to $+\infty$ and the points at these extremes (where the curve terminates on the real axis) are in agreement with Eq. (15). The rotation of the curve is clockwise but the curve does not enclose the critical point (-1,0). Hence, the system is stable but, again, we see that it is not far from instability.

In the next example, we assume that compensation for C_b has been carried too far so that we are left with a residual capacitance that is negative and 10 percent of C_b. The Nyquist diagram for this case is shown in figure 7. The clockwise rotation encloses the (-1,0) point; the system is unstable. Not only does this example show that the assumed operating condition is unfeasible, but, also, it casts further doubt on the practicality of the operation condition illustrated in figure 6. If the gain, A, of the amplifier does not reach its full value immediately after turn-on, the locus of the Nyquist curve will pass through a form similar to that of figure 7 on its way to the final form shown in figure 6. To see this, note that, in Eqs. (12) and (13), when A is small, a and b will have large negative values. Hence, the system could be trapped in an oscillatory regime.

Of the other parameters in Eq. (14) besides a and b, Q_M is of most interest. In the Nyquist diagram, raising Q_M enlarges the loop but it does not change the end points (given by Eq. (15)). Hence, it does not change the stability prediction. The Q_M can become negative, corresponding to negative radiation resistance. To illustrate these cases, figure 8 has been plotted for $Q_M = -8$. The Nyquist loop comes close to enclosing the (-1,0) point but does not quite do so. Although the rotation of the loop has changed from clockwise to counterclockwise, enclosure of the (-1,0) point would still indicate instability (see, for example, reference 13). It appears that negative Q_M has not significantly changed the stability problem.

Imperfect cancellation of G_b is not as deleterious as imperfect cancellation of C_b on the system operation. Thus, variation of the parameter a was found to have little effect on the results. This is predictable from Eq. (14), since the denominator is dominated by the imaginary term.

We conclude from the calculations of this section that the positive-feedback scheme described here operates too close to instability to be practical. Unless someone skilled in stabilization techniques can show how to surmount this difficulty, the method likely will remain unused. In addition to the stability problem, the velocity-control performance deteriorates considerably when realistic variations in C_b are accommodated.

8

NEGATIVE FEEDBACK

An expression for negative velocity feedback can be derived from Eq. (7) by letting $Y_b'' = 0$, indicating perfect cancellation of the blocked admittance, and letting the feedback function, β, be a positive real number. If we then make $A\beta$ large enough, we see that Eq. (7) becomes independent of Z_Y and we have perfect velocity control. The product $A\beta$ has the dimensions of a resistance; so we let $A\beta = R_f$. Equation (7) reduces to

$$\frac{I_{mot}}{E} = \frac{1/\beta}{1 + Z_Y/A\beta} = \frac{A}{R_f + Z_Y} = \frac{A}{R_Y + R_f + jX_Y} . \qquad (16)$$

Negative velocity feedback effectively augments the motional resistance, R_Y, of the transducer and this is the same as augmenting the mechanical resistance, R_M. If the resistance due to feedback, R_f, is made large enough, the variations in Z_Y due to radiation-impedance variations will have negligible effect on I_{mot} or the velocity (since with $Y_b'' = 0$, $V \sim I_{mot}$). In this ideal case, the response, Eq. (16), reduces to $1/\beta = A/R_f$. Using a velocity pickup is equivalent to perfect cancellation of Y_b; hence, the discussion above applies to either of these two cases but only the former is practical since Y_b cannot be cancelled exactly.

When motional-current feedback is used and the compensation for Y_b is not perfect, the feedback factor is

$$J(\omega) = A\beta Y_{in}'' = \omega C_b R_f \left[a + jb + \frac{(\omega_r/\omega)(k^2/(1 - k^2))}{1/Q_M + j(\omega/\omega_r - \omega_r/\omega)} \right] , \qquad (17)$$

where the residual blocked admittance has been expressed in the form

$$Y_b'' = Y_b - Y_b' = \omega C_b (a + jb) .$$

Plots of the closed-loop response are obtained by inserting Eq. (17) in Eq. (5). Those plots presented here are normalized with respect to the ideal response, A/R_f.

A near-ideal case of negative feedback is illustrated in figure 9. The velocity is controlled to better than 1 dB in amplitude and 10 deg in phase over the passband. The conditions $a = 0$ and $b = 0$ were employed; thus, use of a velocity pickup is implied. A plot of the feedback factor, Eq. (17), is given in figure 10, and it reveals that 26 dB of feedback, at resonance, was used to get the good results of figure 9. Figure 10 also shows that there is a phase margin against instability of 90 deg at both high and low frequencies. In a practical design, this phase margin would be exploited in rolling off the loop gain (with auxiliary networks in the feedback loop) at high frequencies so that higher-mode resonances of the transducer would not cause instabilities.

Of course, the response in figure 9 is too flat for good power output in the passband (we have eliminated the useful resonance rise). It would be

necessary to use an input equalizer to restore this in-band rise and properly fill out the power-limit envelope.[14]

In the following examples, the gain factor, $A\beta$, is kept the same as for figures 9 and 10, but the other parameters are varied. First, we consider motional-current feedback with imperfect cancellation of Y_b. Figure 11 shows the feedback factor, $J(\omega)$, when the blocked capacitance cancellation is accomplished to within only 10 percent. The other parameters are the same as for figure 10. The changes caused by the imperfect cancellation are quite pronounced. The phase margin is no worse, but the rising gain at high frequencies could make stability achievement more difficult. The closed-loop response is shown in figure 12. The velocity control now departs 3 dB from the ideal over the passband.

Next, suppose we overcompensate and make the simulator capacitance 10 percent larger than C_b. The feedback factor, $J(\omega)$, for this situation is plotted in figure 13. The phase margin is no worse than before. Once again, rising gain at high frequencies would make stabilization difficult at the higher resonances. The closed-loop response, shown in figure 14, indicates that the velocity control departs 2 dB from the ideal over the passband.

When the radiation resistance becomes negative, the negative-feedback system may fail, as illustrated in figure 15. This is a plot of the feedback factor, $J(\omega)$, for $Q_M = -5$ and $a = b = 0$. We see that the phase angle varies from 90 to 270 deg; this means that on a Nyquist diagram the (-1,0) point would be encircled in the counterclockwise direction. The system is, therefore, unstable.

For very heavy radiation loading, the velocity control is poor, as illustrated in figure 16. This is a plot of closed-loop response for $Q_M = 0.4$ and $a = b = 0$. The velocity control departs over 4 dB from the ideal over the passband.

We conclude from the examples of this section that the full potential of negative feedback will be realized only if a velocity pickup is used. When motional-current feedback is employed, the limitations of the Y_b-simulator circuit will cause considerable loss of performance. If negative radiation resistances are avoided, the prospects for synthesizing a stable system appear good.

CARSON VELOCITY CONTROL

Carson's approach to velocity control is to make the mechanical driving-point impedance (at the projector's radiating face) become large at the frequency where velocity control is most desired. Radiation impedance variations, then, will have little effect on the velocity, as can be appreciated by replacing the transducer and its driving system by a mechanical Thévenin circuit, as shown in figure 1c. Here, Z_{Thev} is the mechanical driving-point impedance of the system in figure 1a, with $E = 0$. We consider only the parallel-tuned case. The impedance, Z_{Thev}, will have a pole at the parallel-tuned

frequency, $\omega_b = \sqrt{1/L_b C_b}$, if the amplifier has infinite output impedance. Thus, a current amplifier is desired when parallel tuning is used.

To achieve Carson velocity control with the circuit of figure 1, we omit the Y_b-simulator and make the feedback gain, $A\beta$, large, with β real. These steps convert the voltage amplifier to a current amplifier. A tuning inductor, L_b, is placed in parallel with Y_b. There is no stability problem in the Carson method, since electromechanical feedback is not employed. Negative radiation resistances could still be troublesome, however, especially if the amplifier is not fully reversible.

To analyze this system (with $Y_b' = 0$), we use Eq. (7),

$$\frac{I_{mot}}{E} = \frac{1/\beta}{1 + Z_Y(Y_b + 1/A\beta)} , \qquad (18)$$

with the understanding that Y_b now includes the parallel-tuning inductor, L_b. Velocity control will be achieved if the term in parentheses in the denominator is made small. The second term in the parentheses can be made negligible by using a large feedback factor, $A\beta$, in the amplifier portion of the system. The first term in the parentheses is small at the parallel-resonance frequency, ω_b. Because the desired condition exists only near this resonance, Carson velocity control tends to be narrowband.

After the $1/A\beta$ term is dropped, Eq. (18) can be written as

$$\frac{I_{mot}}{E} = \frac{1/\beta}{1 + Z_Y Y_b} = \frac{1/\beta}{1 + Z_Y \omega C_b \left[\frac{\omega_b/\omega}{Q_b} + j\left(1 - \frac{\omega_b^2}{\omega^2}\right) \right]} , \qquad (19)$$

where $Q_b = \omega_b C_b / G_b$ and G_b includes the inductor loss, as well as the dielectric loss, at the frequency ω_b. It can be shown that $|Z_Y \omega C_b| \sim (1 - k^2)/k^2$; hence, the bandwidth for Carson velocity control increases with increased coupling factor.

In the examples illustrating Carson velocity control, Q_b is chosen to be 30 and the parallel resonance is made to coincide with the transducer's mechanical resonance when operating alone ($\omega_b = \omega_0$). The first example is for $Q_M = 5$; a plot of Eq. (19) relative to perfect velocity control ($Y_b = 0$) is given in figure 17. At the tuned frequency, $\omega_b = \omega_0$, the velocity control is perfect. Over the full passband of the transducer, however, the velocity control departs 8 dB from the ideal. The phase control appears especially bad, deviating as much as 130 deg in the passband.

A high-Q_M case is shown in figure 18. The velocity control at the edges of the passband is worse than before. However, both figures 18 and 17 show a 30 percent bandpass region, extending from 0.95 ω_0 to 1.25 ω_0, where the velocity control is reasonably good. The next example is a low-Q_M case, shown in figure 19. It exhibits poor velocity control. Finally, an example of

negative radiation resistance is shown in figure 20. With Q_M = -5, the velocity control is worse than for Q_M = +5, but only moderately so.

The double-peaked response appearing in figure 17 would seldom be considered desirable and it would not be good for maximum power output because the voltage in the region of the two peaks would be too high. Evidently, an input equalizer should be used to reshape the response so that it would fill out the power-limit envelope more advantageously. Unfortunately, an equalizer tailored to the response of figure 17 would fail to do its job if beam steering caused this projector to become heavily loaded, as in figure 19, for example.

The examples of this section lead to the conclusion that velocity-control bandwidth using Carson's approach[1] is considerably less than the transmission-loss bandwidth defined by Mason.[15] For narrowband systems, the Carson approach is a preferred choice because of its simplicity and assured stability. It would also be good in switched-frequency systems if the inductor could be switched to maintain resonance every time the signal frequency was switched.

GENERAL CONCLUSIONS

Positive-feedback systems, such as the system suggested by Design Automation, Inc., appear to operate too close to instability to be practical.

Negative-feedback systems employing velocity sensors appear to have a great deal to offer and should be investigated further. Critical items to be studied include avoidance of instabilities at the higher transducer resonances and achievement of low crosstalk between the sensor leads and the transducer power leads. Use of negative feedback is contingent on the ability to design arrays with no negative radiation resistances.

Negative-feedback systems using motional-current extraction are of doubtful utility because of the difficulty of cancelling accurately the blocked capacitance of the transducer. However, the problem of compensating for variations of C_b with voltage, temperature, and pressure when implementing such a system deserves further study.

Carson velocity control remains attractive for narrowband systems, but no avenues appear open to extend its bandwidth. For switched-frequency sonars, methods for dynamically changing the electrical tuning of the transducer should be studied.

All velocity-control schemes distort the frequency response of the system in undesirable ways. Hence, one should attempt to reshape the response so that it properly fills out the power-limit envelope of the projector, by the use of input equalizers or other means.

The effectiveness of the velocity-control measures and the distortions they cause in the frequency response depend strongly on the radiation impedance presented to the projector being examined. Hence, for future studies to

be complete, they should encompass all projector positions in the array, all steering angles and shading functions, and all frequencies in the passband. The examples given here represent a very sparse sampling of the possible cases.
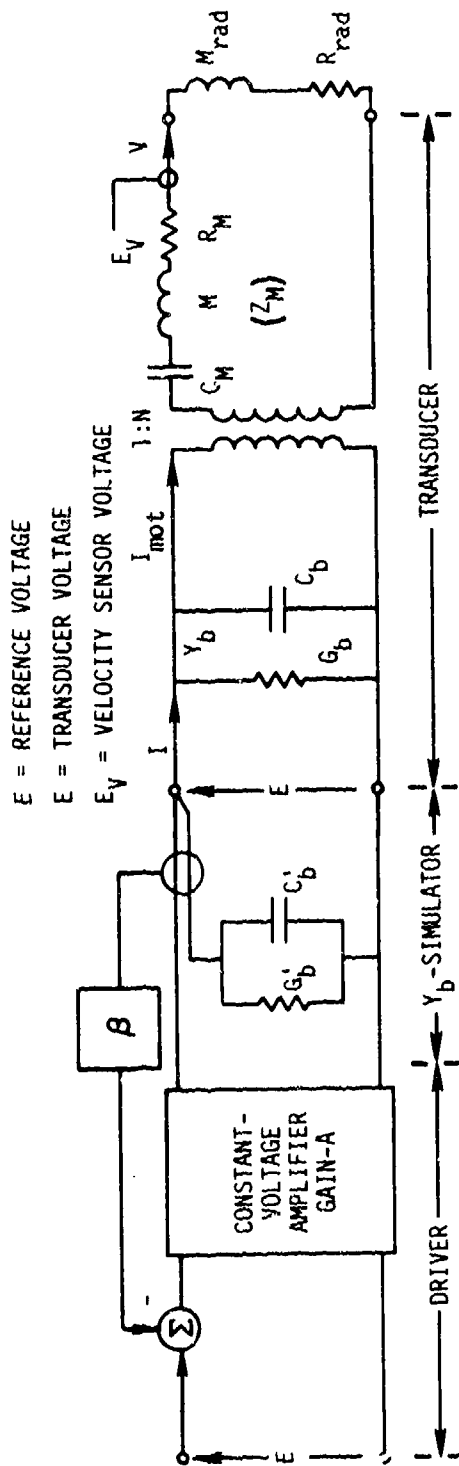
E = REFERENCE VOLTAGE

E = TRANSDUCER VOLTAGE
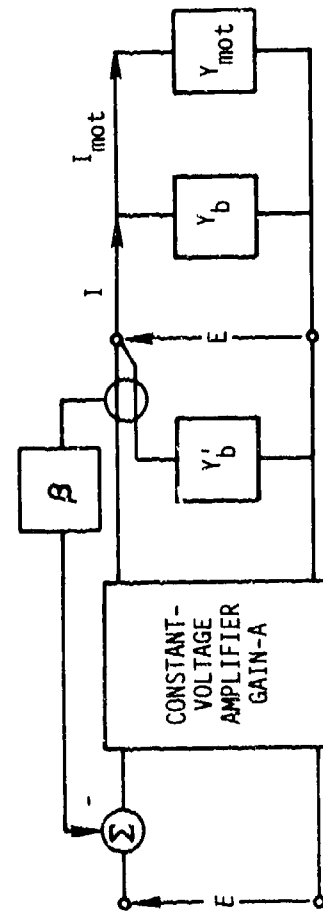
E_V = VELOCITY SENSOR VOLTAGE

Figure 1a. Electromechanical

Figure 1b. Purely Electrical
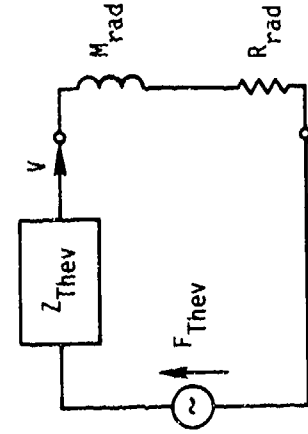
Figure 1c. Mechanical Thévenin Circuit
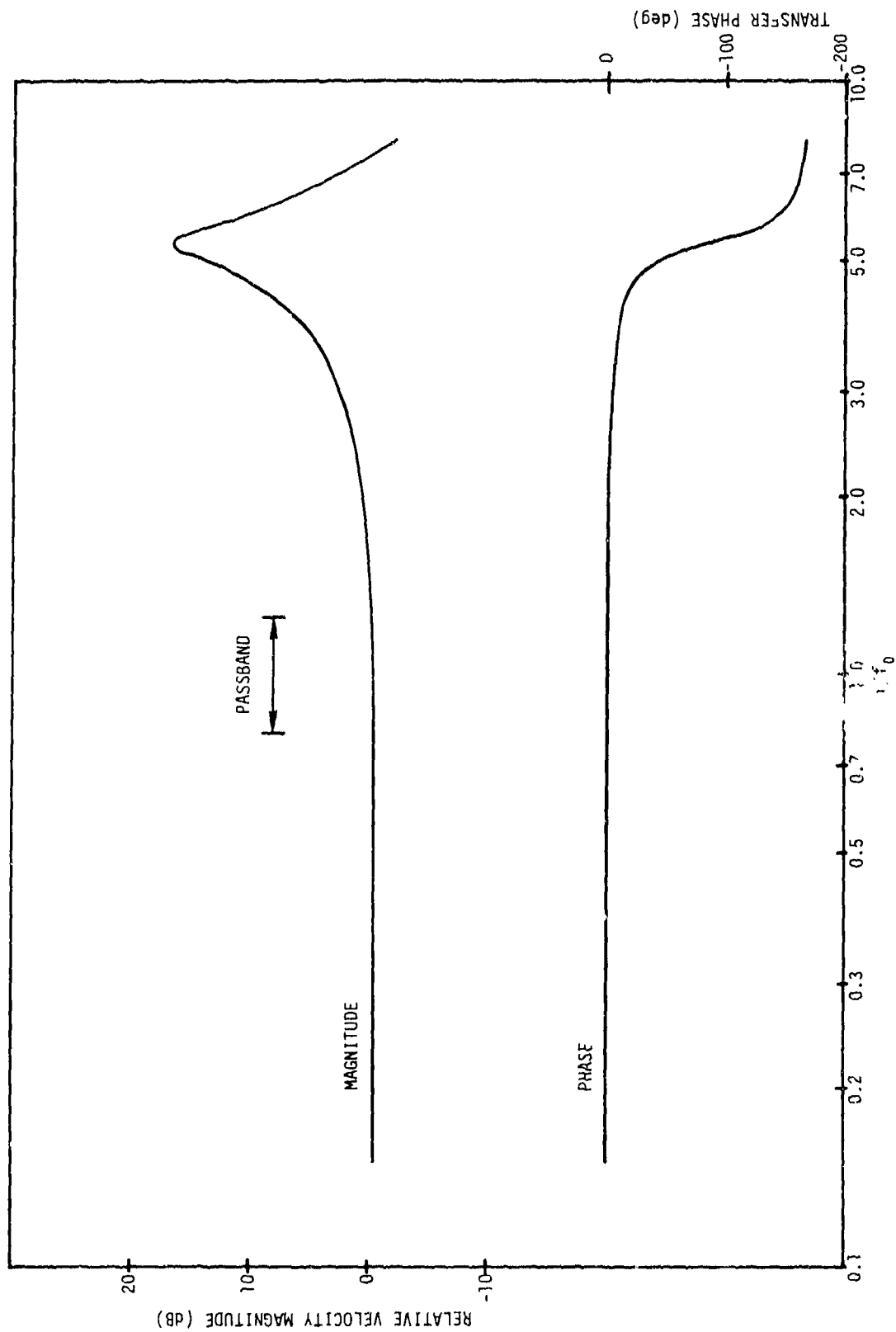
Figure 1. Representations of the Projector System

Figure 2. Closed-Loop Response V/E Relative to Perfect Velocity Control
(a = 0.001, b = 0.01, Q_M = 5, and f_r/f_0 = 1.2)
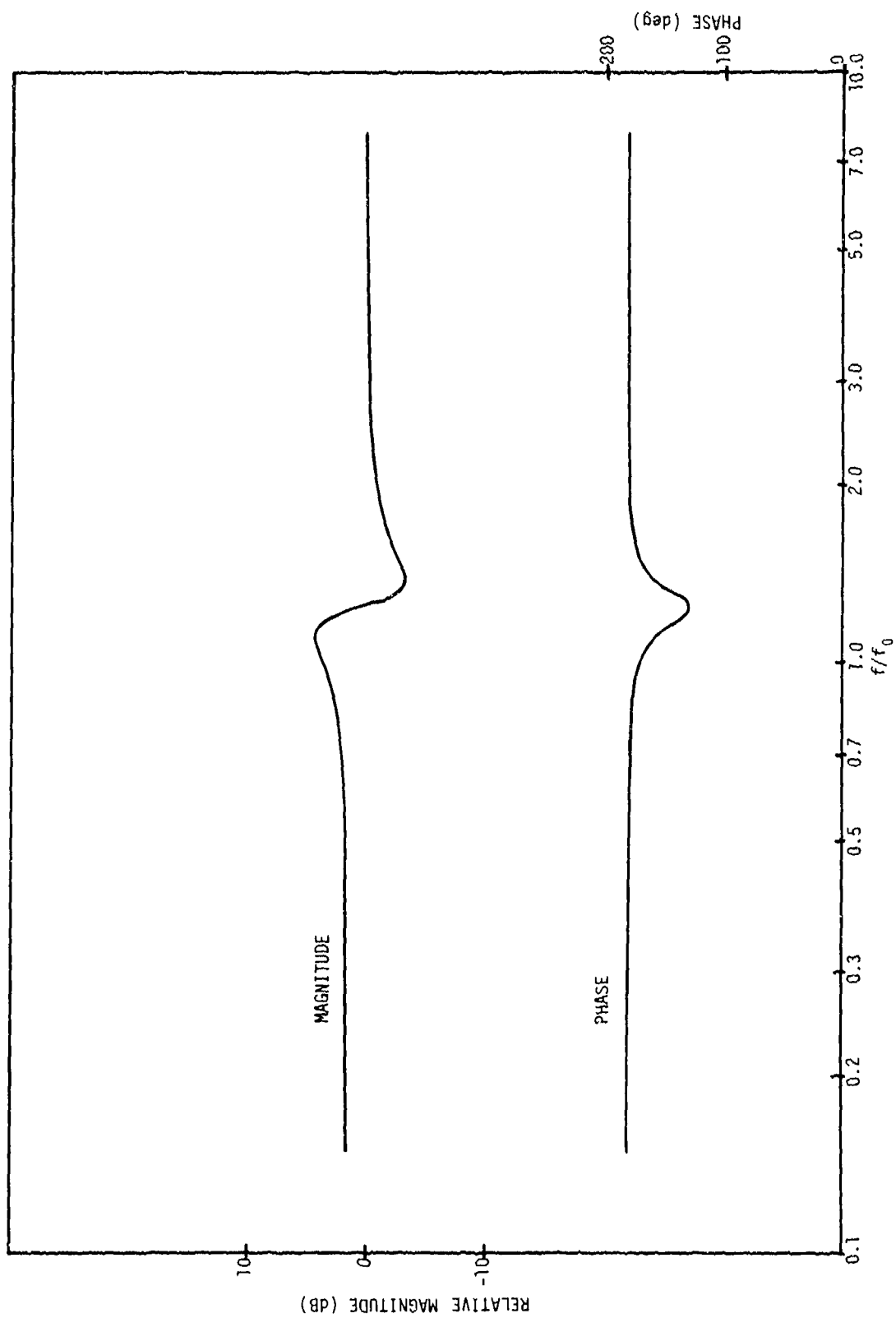
Figure 3. Positive Feedback, Magnitude and Phase of Feedback Factor $J(\omega)$
($a = 0.001$, $b = 0.01$, $Q_M = 5$, and $f_r/f_0 = 1.2$)
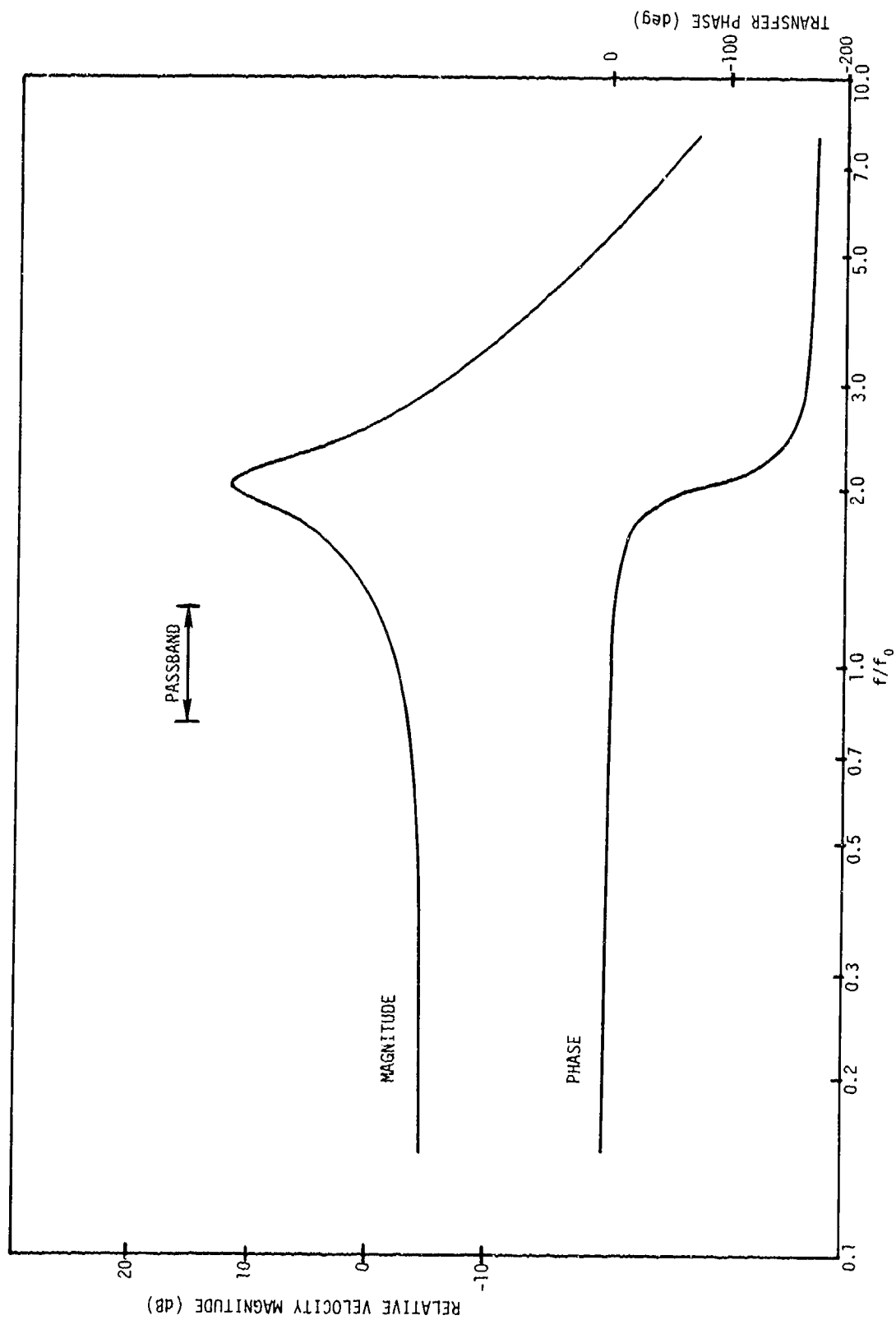
Figure 4.   Closed-Loop Response V/E Relative to Perfect Velocity Control
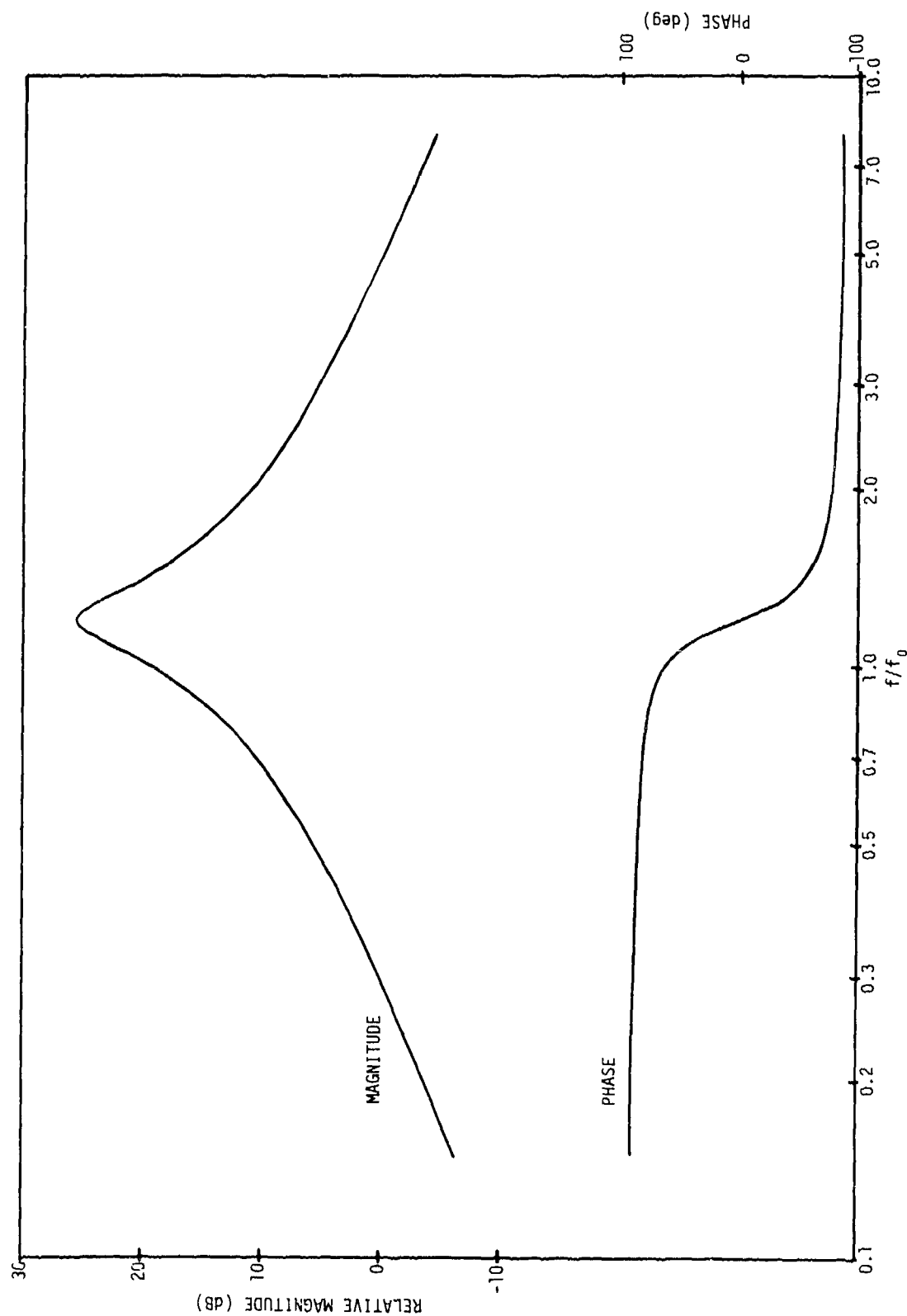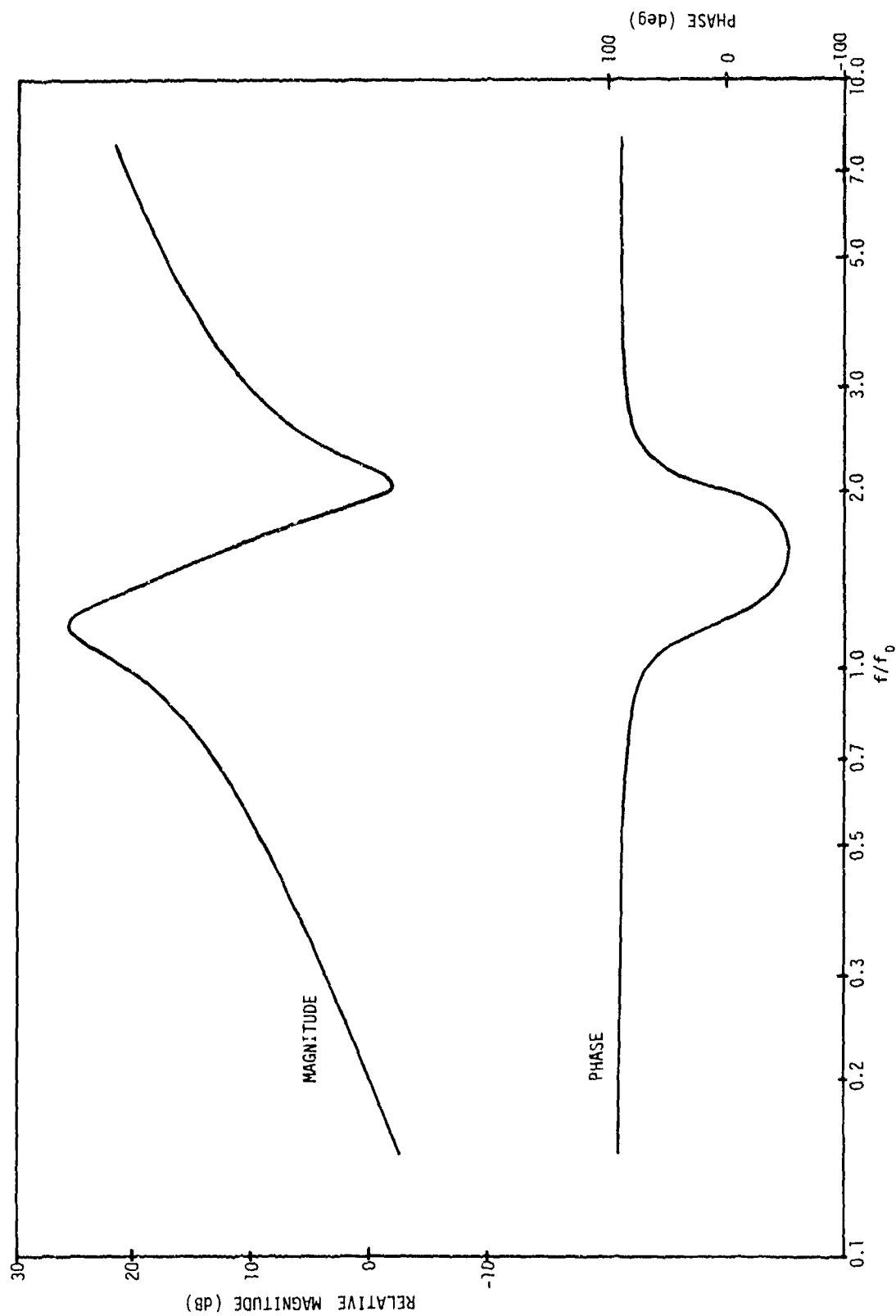(a = 0.005, b = 0.1, Q_M = 5, and f_r/f_0 = 1.2)
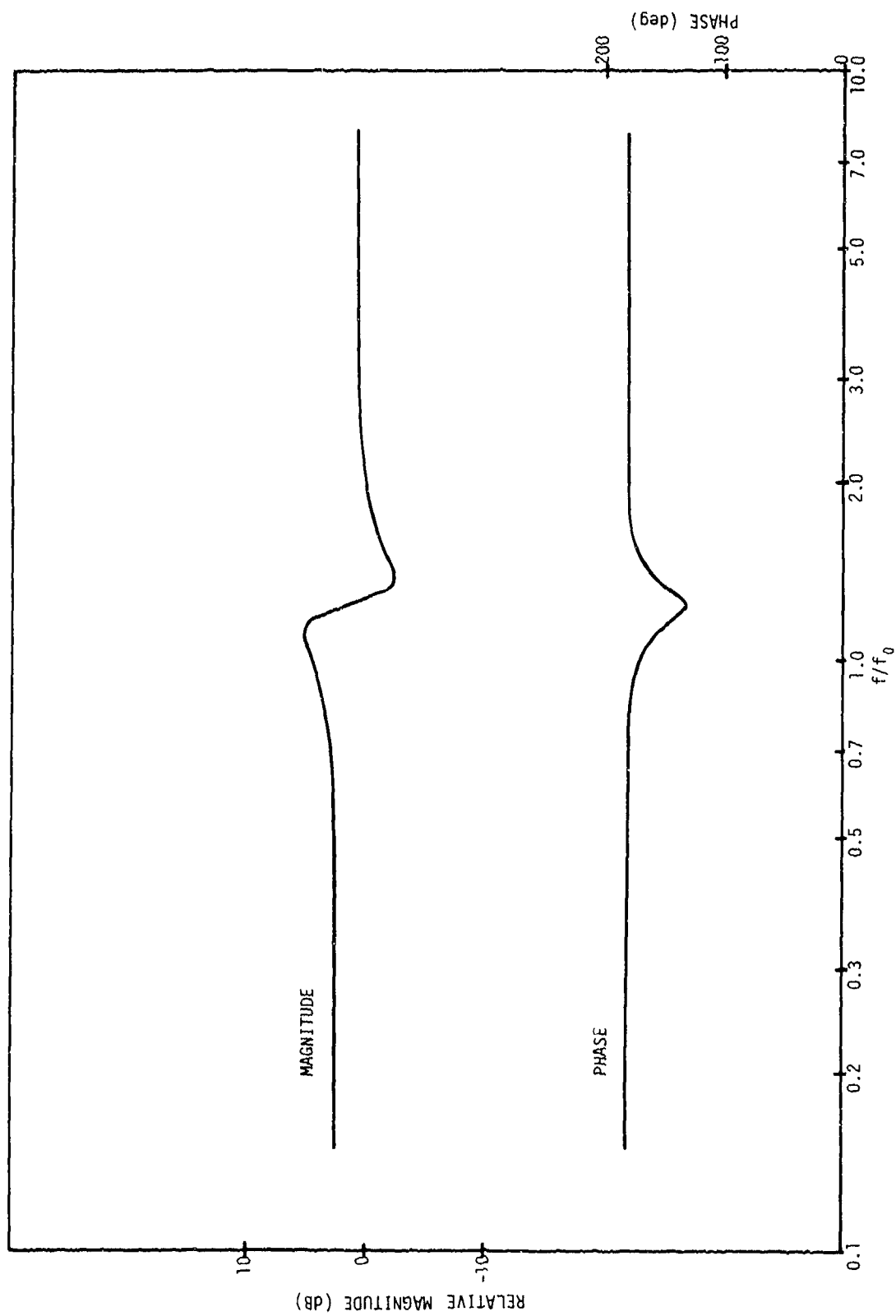
Figure 5. Positive Feedback, Magnitude and Phase of Feedback Factor $J(\omega)$
($a = 0.005$, $b = 0.1$, $Q_M = 5$, and $f_r/f_0 = 1.2$)
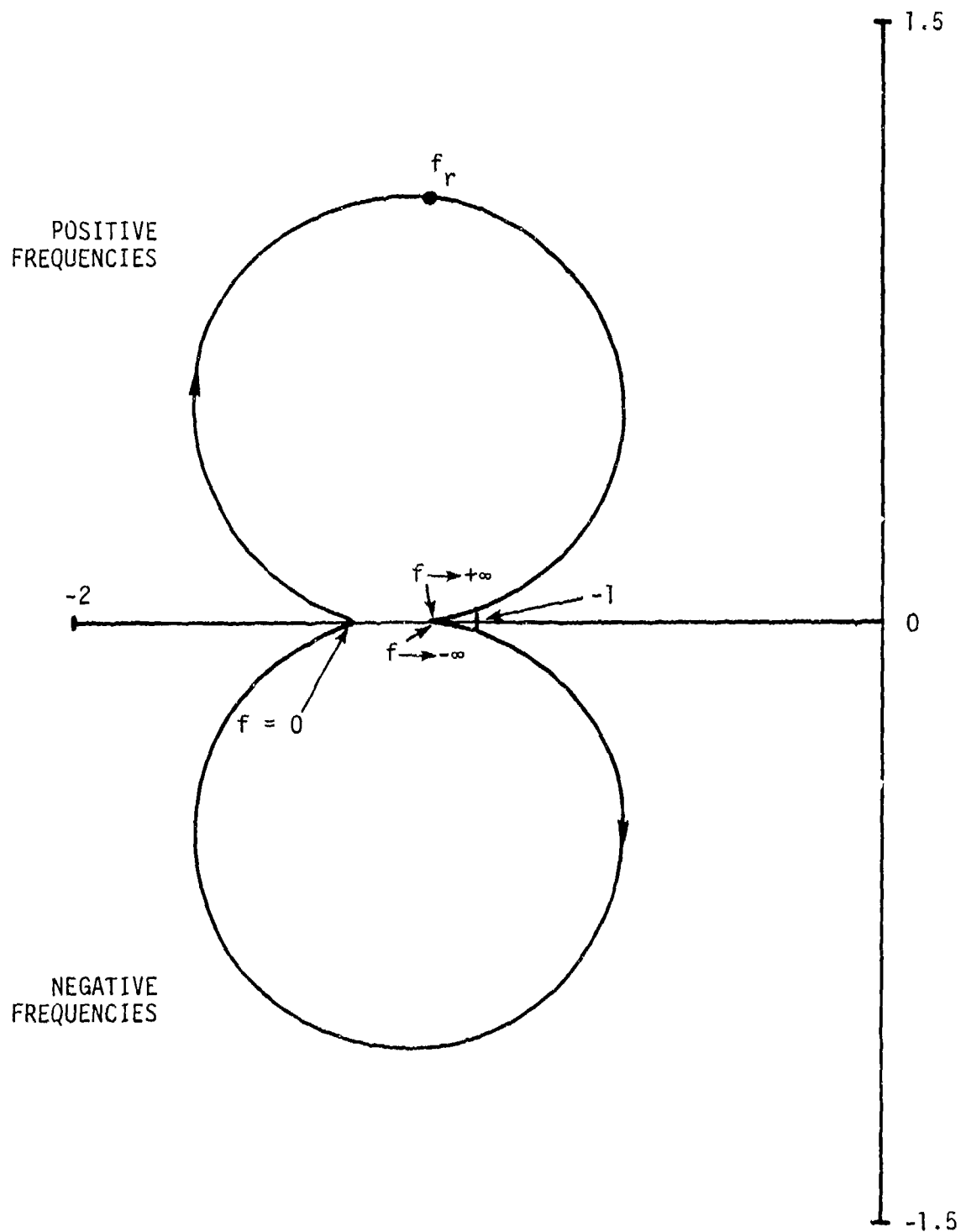
Figure 6.   Positive Feedback, Nyquist Diagram (a = 0.005, b = 0.1, Q_M = 5, and f_r/f_0 = 1.2)
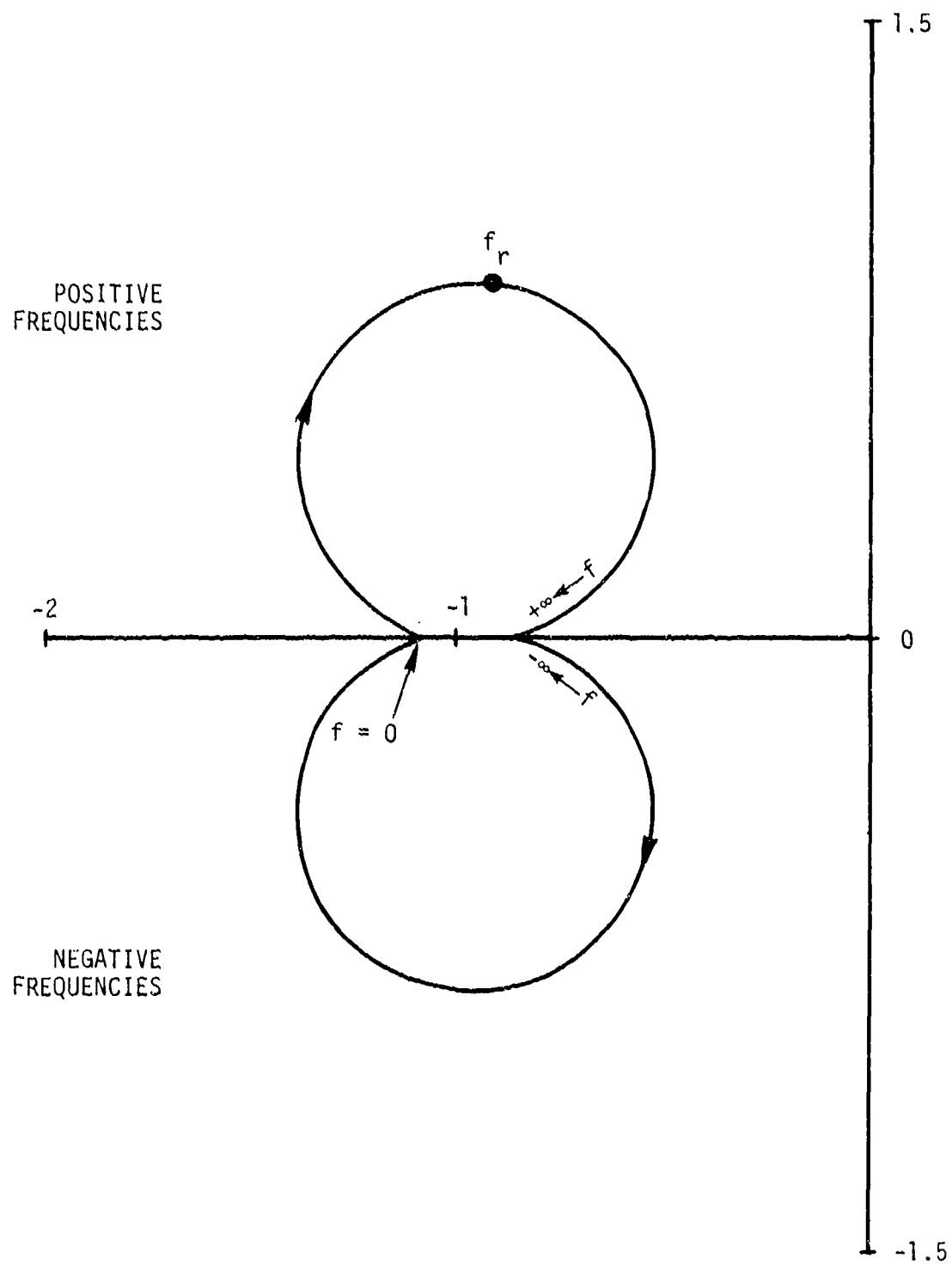
Figure 7. Positive Feedback, Nyquist Diagram (a = -0.005,
b = -0.1, Q_M = 5, and f_r/f_0 = 1.2)
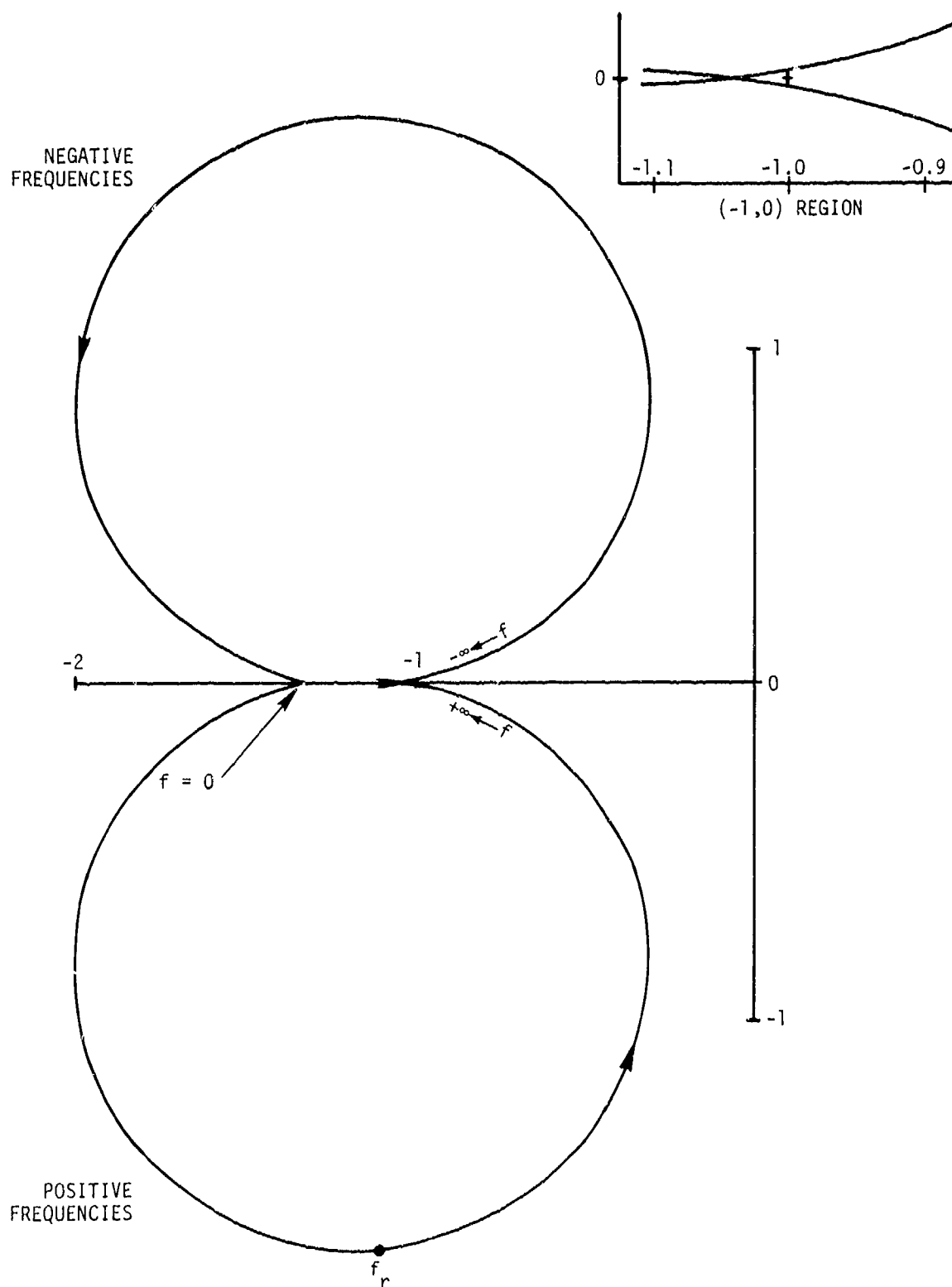
Figure 8. Positive Feedback, Nyquist Diagram (a = 0.005, b = 0.1, Q_M = -8, and f_r/f_0 = 1.2)
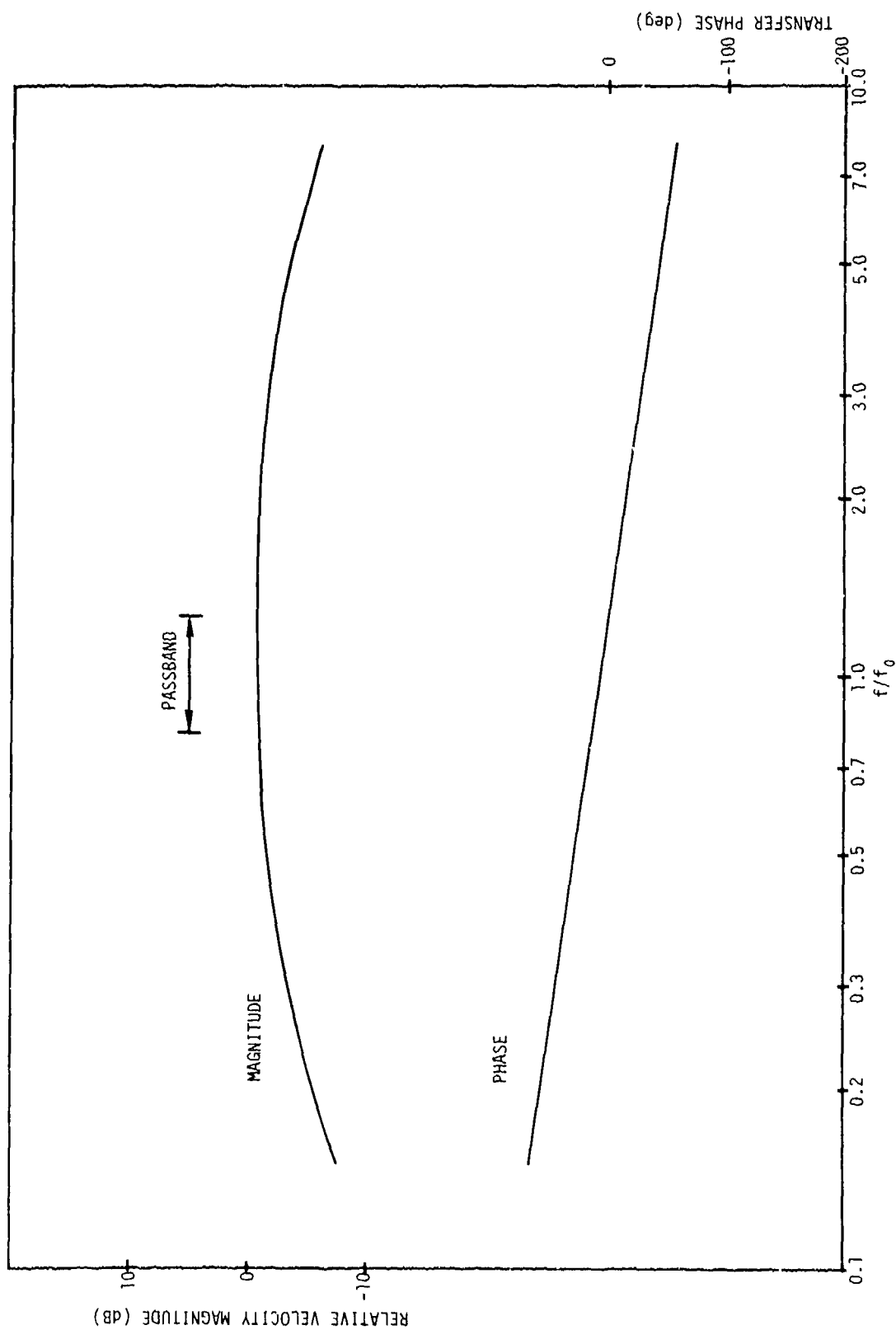
Figure 9. Closed-Loop Response V/E Relative to Perfect Velocity Control
$(a = 0, b = 0, Q_M = 5, f_r/f_0 = 1.2,$ and $\omega_r C_b R_f = 20)$

Figure 10. Negative Feedback, Magnitude and Phase of Feedback Factor $J(\omega)$
($a = 0$, $b = 0$, $Q_M = 5$, $f_r/f_0 = 1.2$, and $\omega_r C_b R_\varepsilon = 20$)

Figure 11. Negative Feedback, Magnitude and Phase of Feedback Factor $J(\omega)$ ($a = 0.005$, $b = 0.1$, $Q_M = 5$, $f_r/f_0 = 1.2$, and $\omega_r C_b R_f = 20$)
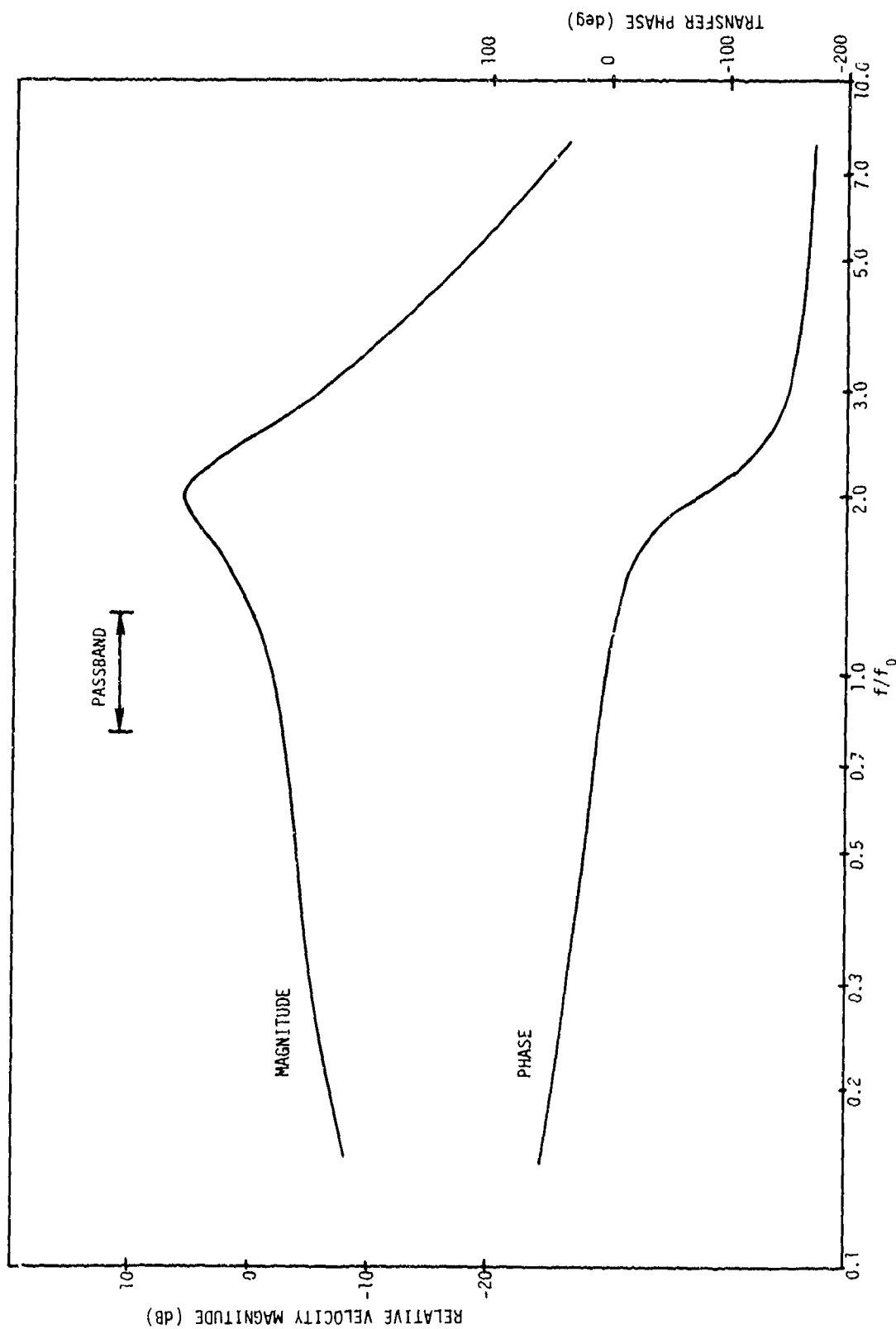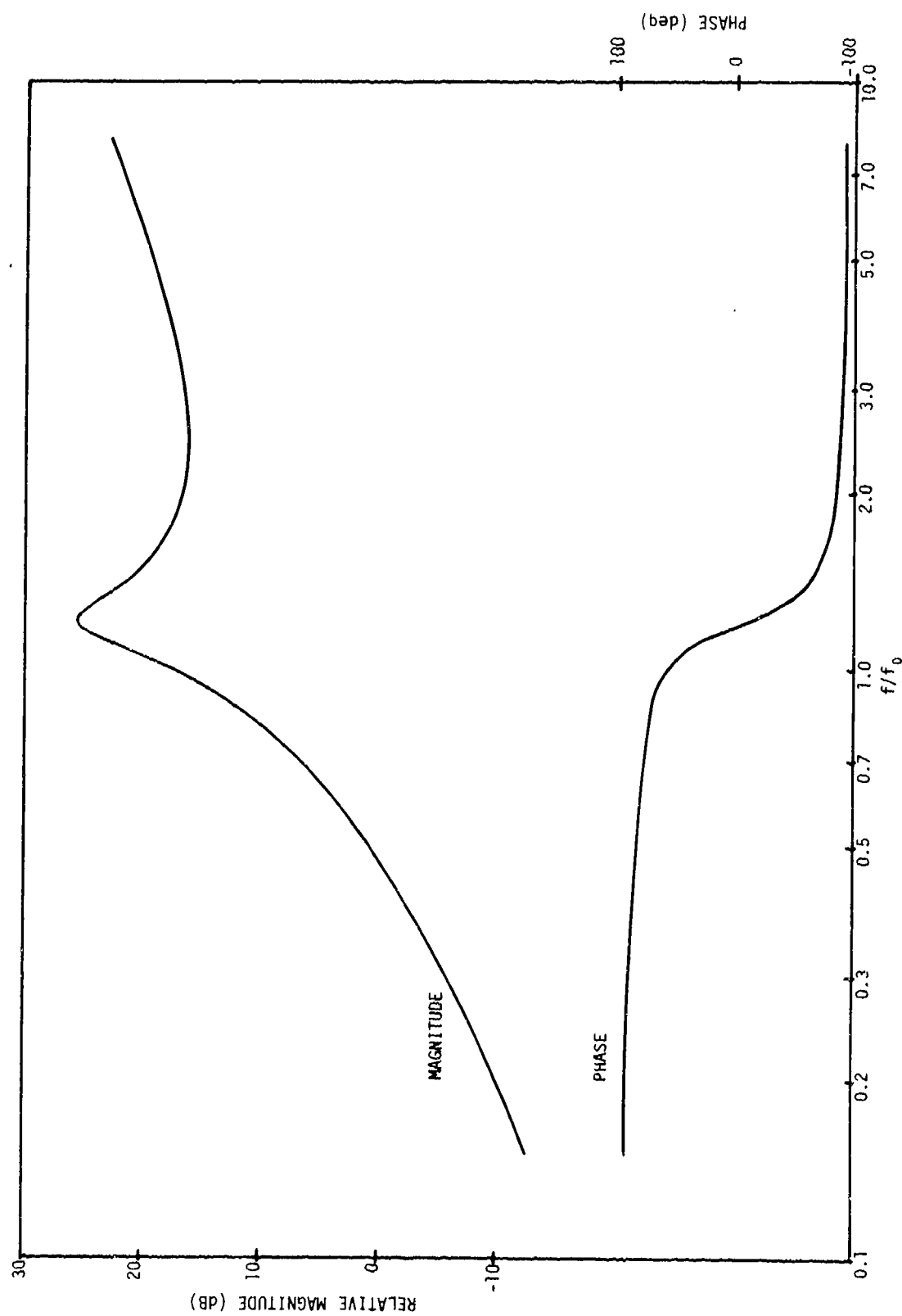
Figure 12.   Closed-Loop Response V/E Relative to Perfect Velocity Control
(a = 0.005, b = 0.1, Q_M = 5, f_r/f_0 = 1.2, and $\omega_r C_b R_f$ = 20)

Figure 13. Negative Feedback, Magnitude and Phase of Feedback Factor $J(\omega)$
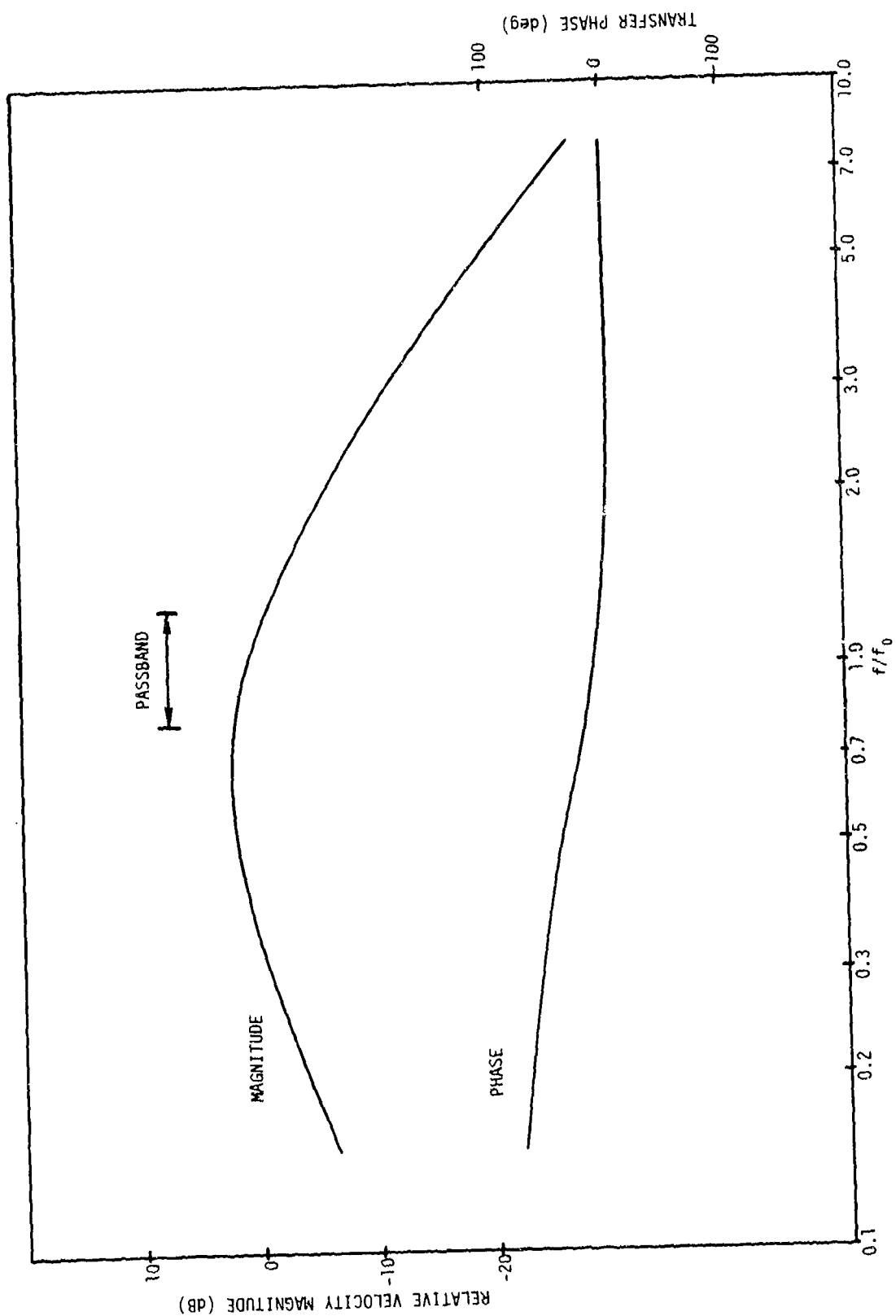($a = -0.005$, $b = -0.1$, $Q_M = 5$, $f_r/f_0 = 1.2$, and $\omega_r C_b R_f = 20$)

Figure 14. Closed-Loop Response V/E Relative to Perfect Velocity Control
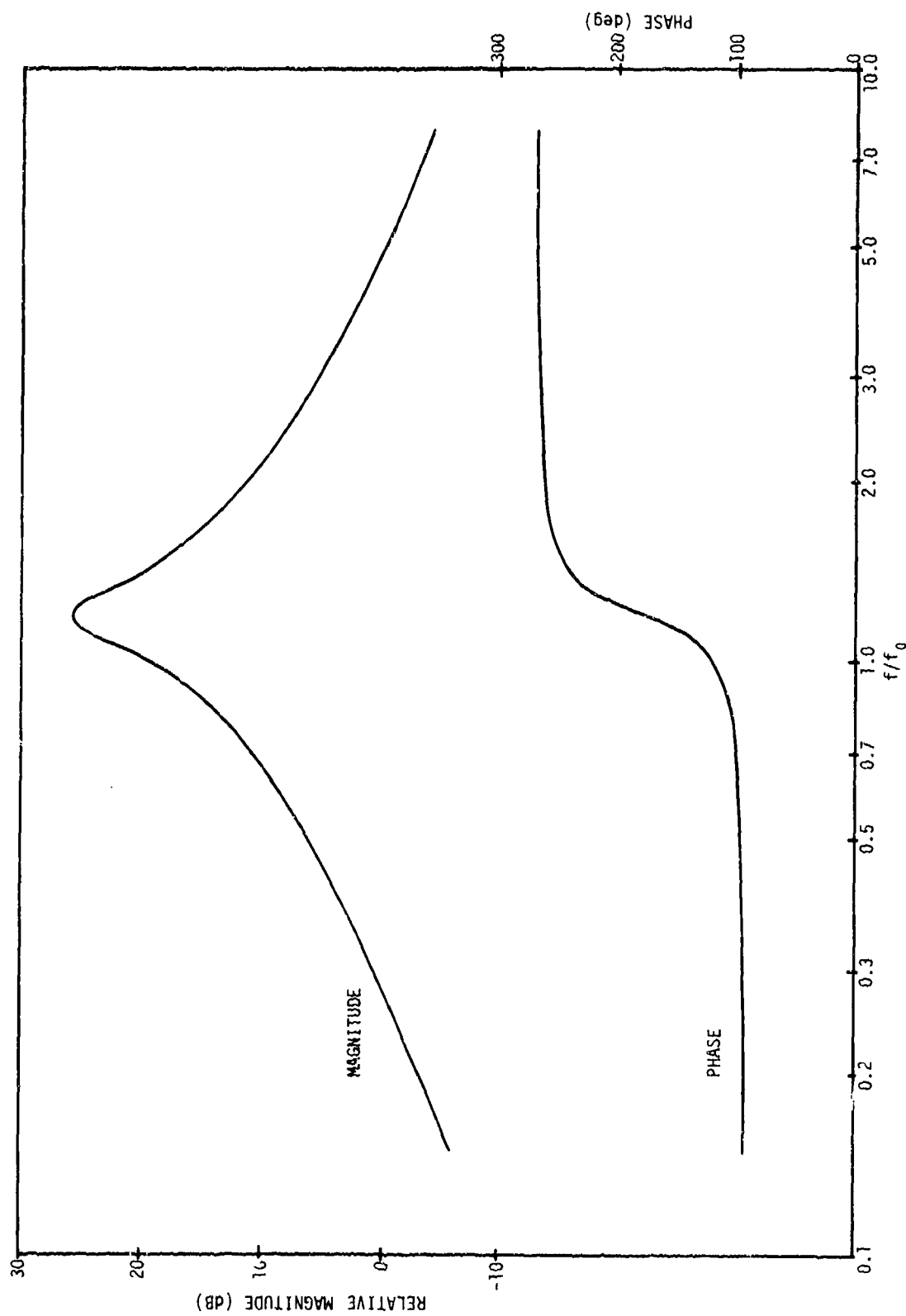($a = -0.005$, $b = -0.1$, $Q_M = 5$, $f_r/f_0 = 1.2$, and $\omega_r C_b R_f = 20$)

Figure 15. Negative Feedback, Magnitude and Phase of Feedback Factor $J(\omega)$
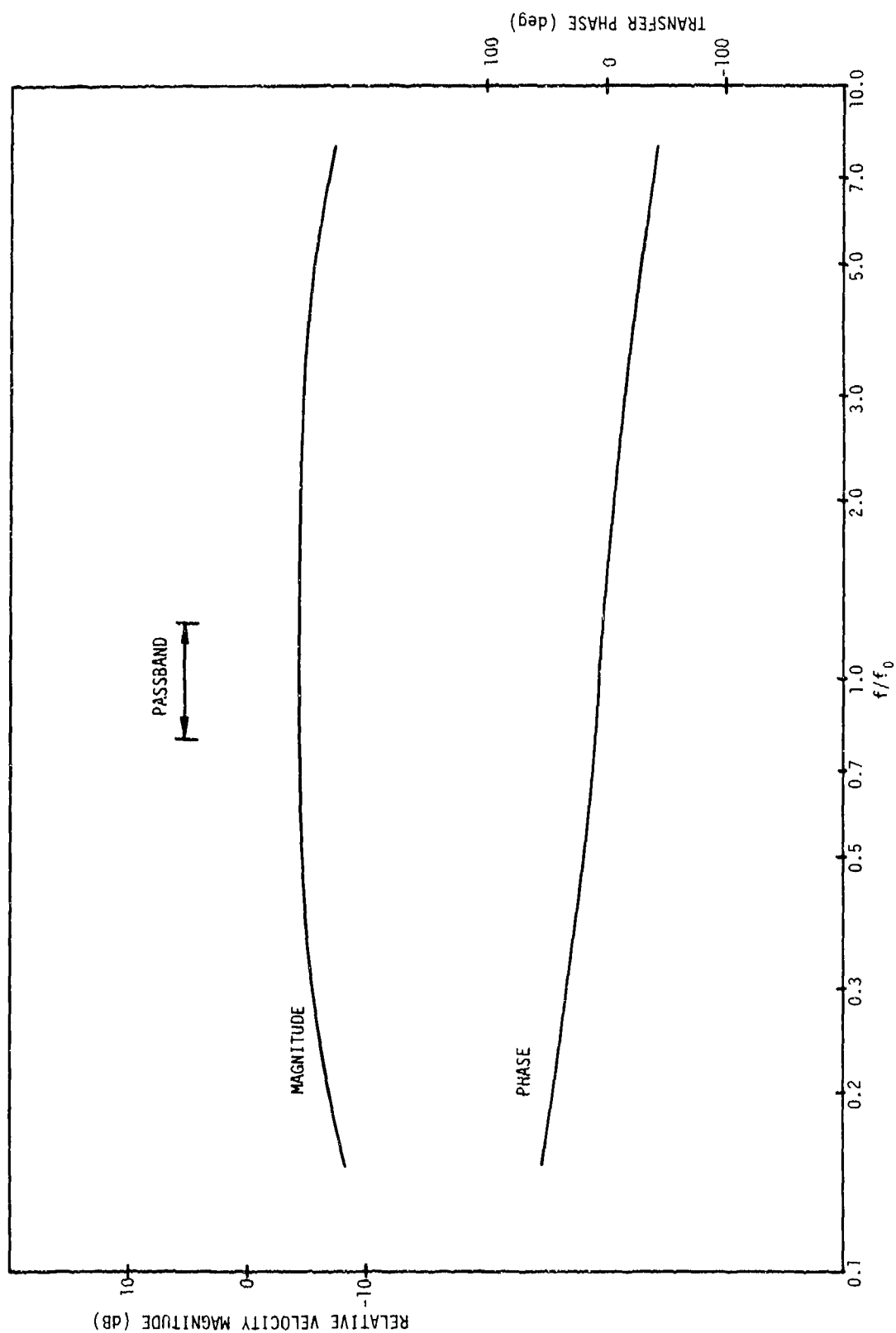$(a = 0, b = 0, Q_M = -5, f_r/f_0 = 1.2, \text{ and } \omega_r C_b R_f = 20)$

Figure 16. Closed-Loop Response V/E Relative to Perfect Velocity Control
(a = 0, b = 0, Q_M = 0.4, f_r/f_0 = 1.2, and $\omega_r C_b R_f$ = 20)

Figure 17. Carson Velocity Control, Response V/E Relative to Perfect Control
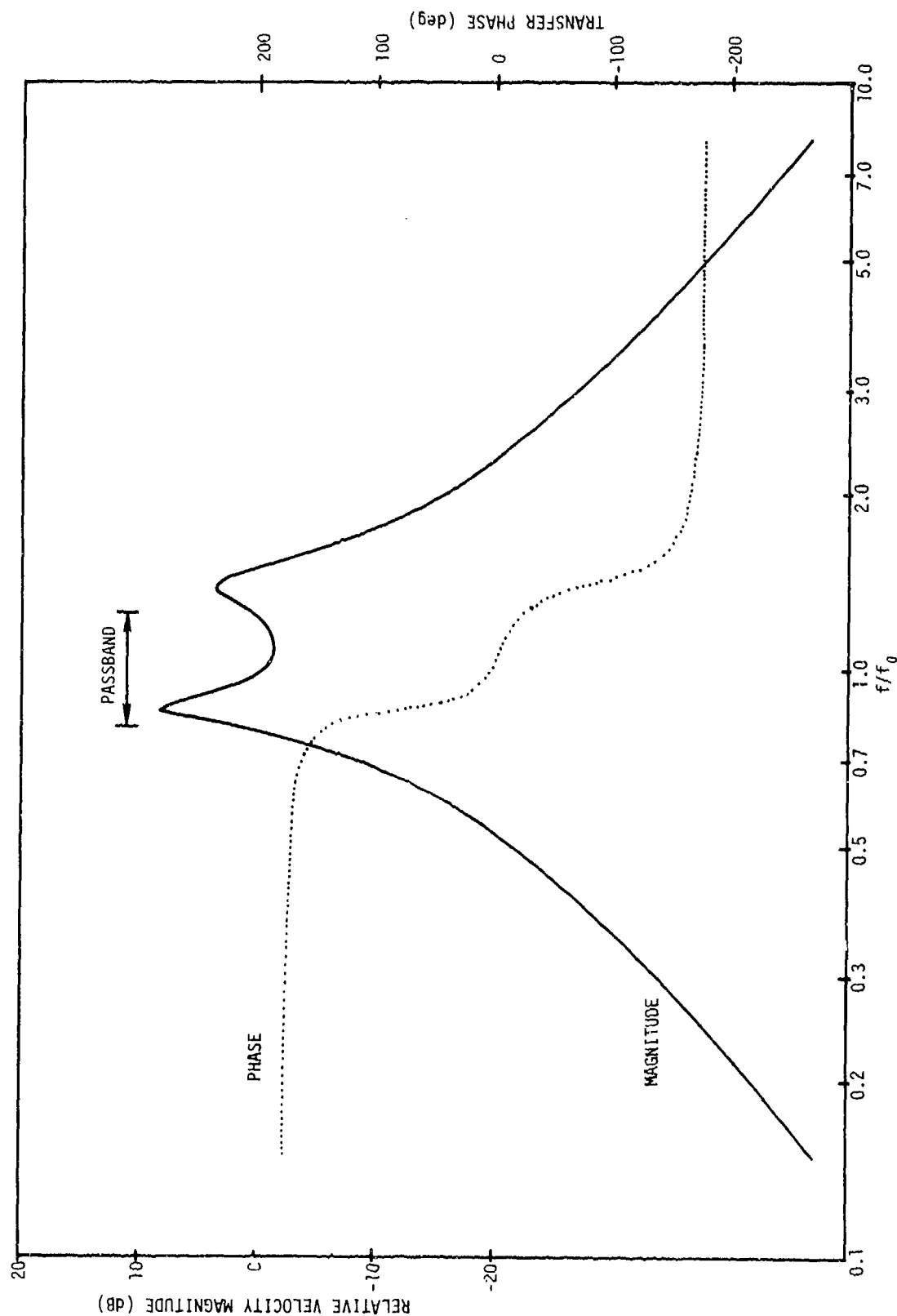($Q_M = 5$, $Q_b = 30$, $f_r/f_0 = 1.2$, and $f_b/f_0 = 1$)

Figure 18. Carson Velocity Control, Response V/E Relative to Perfect Control $(Q_M = 30, Q_b = 30, f_r/f_0 = 1.2, \text{ and } f_b/f_0 = 1)$
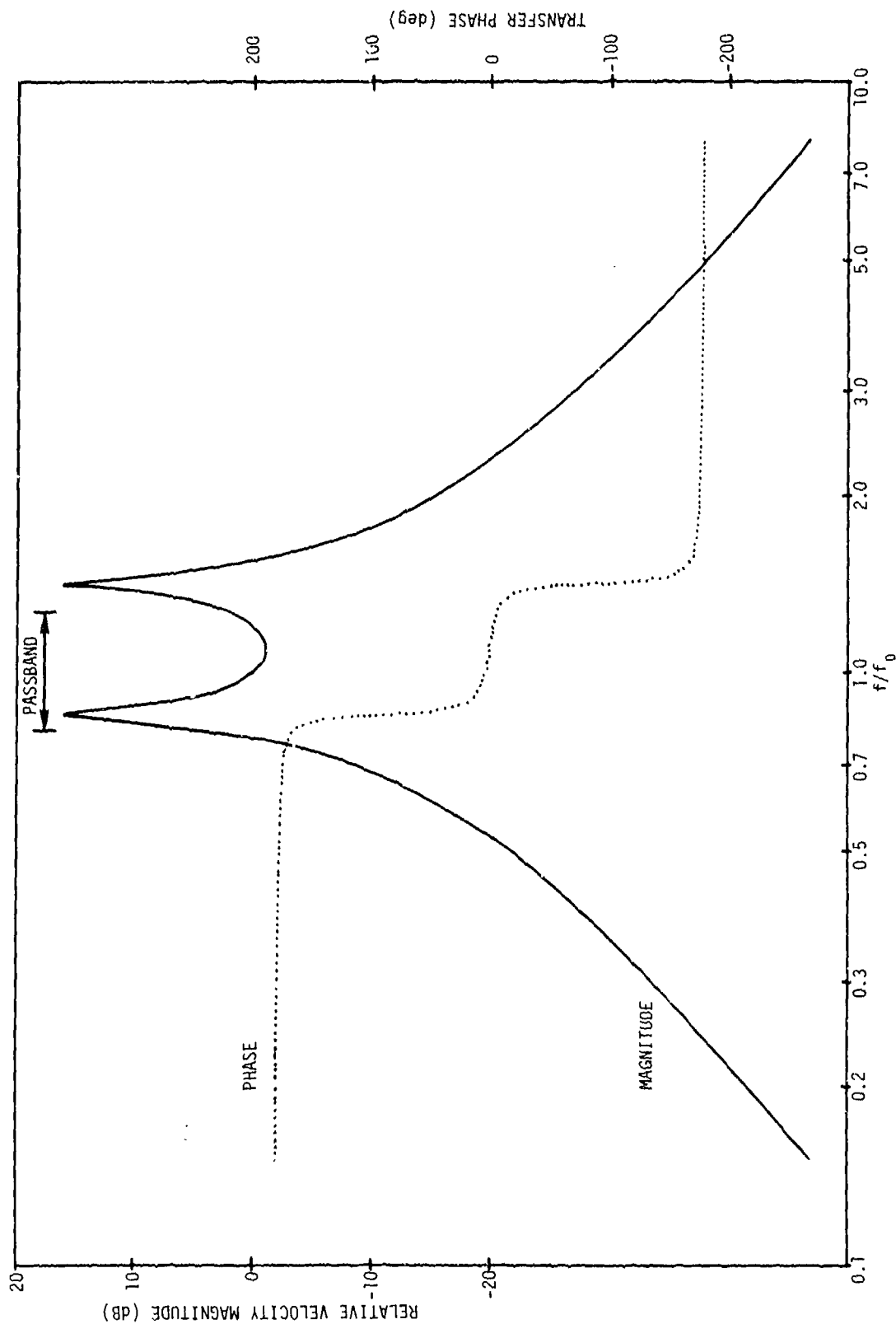
Figure 19. Carson Velocity Control, Response V/E Relative to Perfect Control
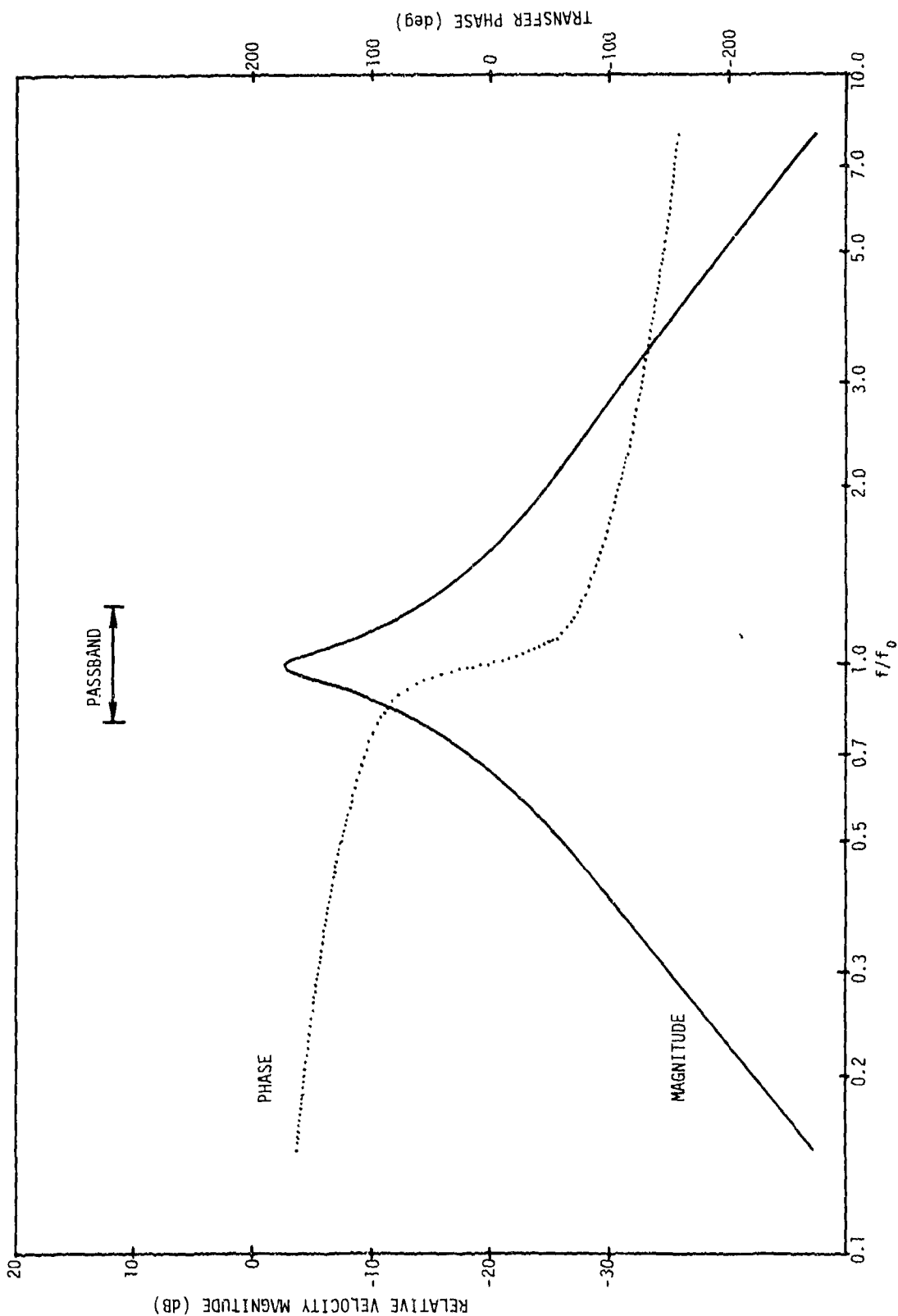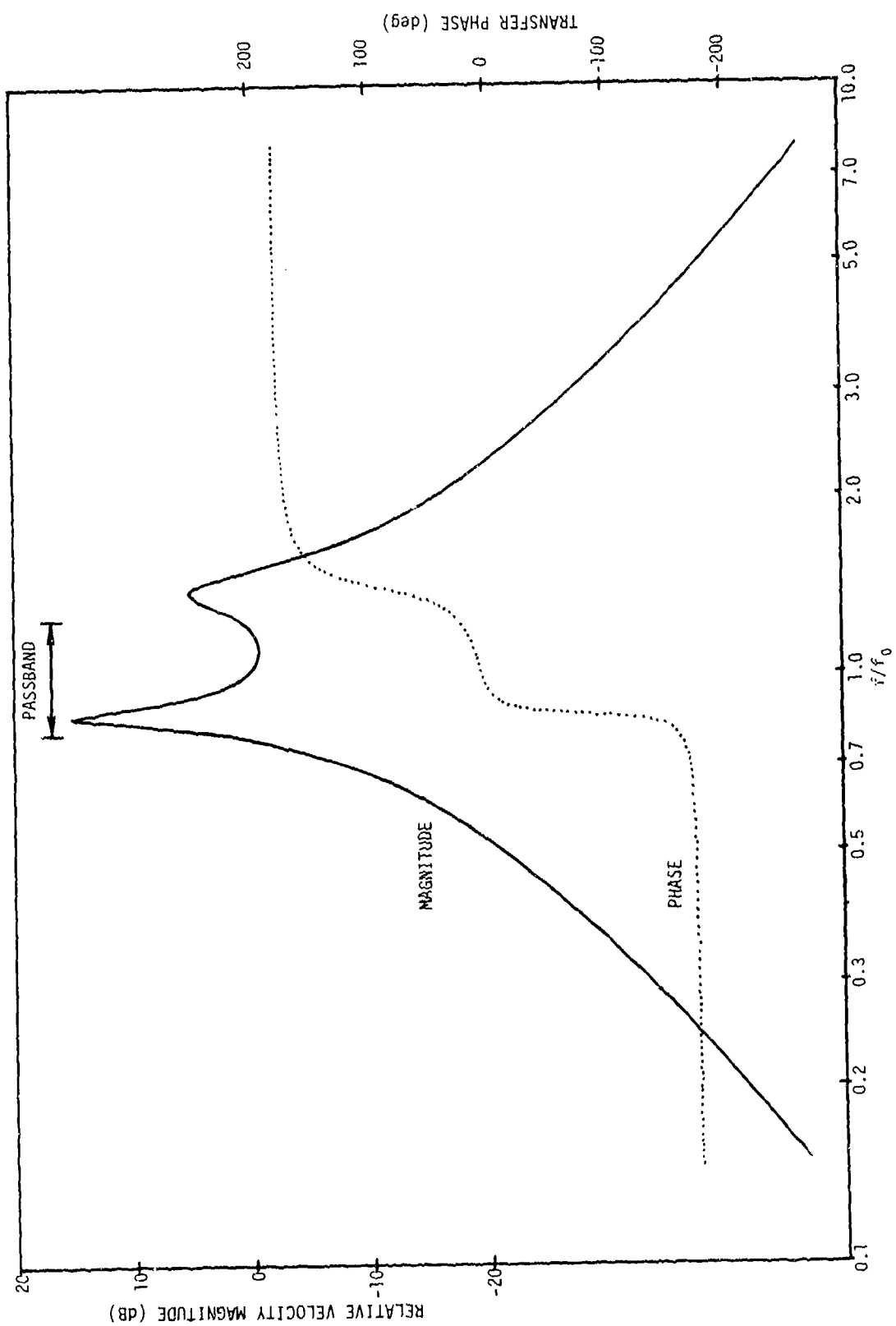($Q_M = 0.4$, $Q_b = 30$, $f_r/f_0 = 1.2$, and $f_b/f_0 = 1$)

Figure 20. Carson Velocity Control, Response V/E Relative to Perfect Control
($Q_M = -5$, $Q_b = 30$, $f_r/f_0 = 1.2$, and $f_b/f_0 = 1$)

REFERENCES

1. D. L. Carson, "Diagnosis and Cure of Erratic Velocity Distributions in Sonar Projector Arrays," Journal of the Acoustical Society of America, vol. 34, 1962, pp. 1191-1196.

2. L. Vieth and C. F. Wiebusch, Journal of the Society of Motion Picture Engineering, January 1938.

3. H. F. Olson, Acoustical Engineering, D. Van Nostrand, NY, 1957, p. 168.

4. R. E. Werner, "Effect of a Negative Impedance Source on Loudspeaker Performance," Journal of the Acoustical Society of America, vol. 29, 1957, pp. 335-340.

5. H. W. Holdaway, "Design of Velocity-Feedback Transducer Systems for Stable Low-Frequency Behavior," IEEE Transactions, vol. AU-11, 1963, pp. 155-173.

6. J. A. Klaassen and S. H. deKoning, "Motional Feedback with Loudspeakers," Philips Technical Review, vol. 29, 1968, pp. 148-157.

7. C. M. van der Burgt, "Motional Positive Feedback Systems for Ultrasonic Power Generators," IEEE Transactions, vol. UE-10, 1963, pp. 2-19.

8. J. V. Bouyoucos and R. L. Selsam, "Very-Low Frequency Broadband Hydroacoustic Sound Source," Journal of Underwater Acoustics, vol. 25, 1975, pp. 585-592.

9. R. S. Woollett, Underwater Helmholtz Resonator Transducers: General Design Principles, NUSC Technical Report 5633, Naval Underwater Systems Center, New London, CT, 5 July 1977, AD-A043359.

10. M. Greenspan, "Transducer Measurements: Use of the Current Probe," Journal of the Acoustical Society of America, vol. 53, 1973, pp. 1186-1187.

11. NUSC Memo 1323-342 from R. S. Woollett to A. W. Ellinthorpe, "Representation of Acoustic Interactions in Projector Arrays," Naval Underwater Systems Center, New London, CT, 1 June 1981.

12. "Engineering Study of a Sonar Transducer Drive System," Report to General Dynamics Corp., Electric Boat Division, by Design Automation, Inc., Lexington, MA, 13 June 1980.

13. H. Chestnut and R. W. Mayer, Servomechanisms and Regulating System Design, 2nd ed., John Wiley and Sons, NY, 1959, p. 145.

14. R. S. Woollett, "Basic Problems Caused by Depth and Size Constraints in Low-Frequency Underwater Transducers," Journal of the Acoustical Society of America, vol. 68, 1980, pp. 1031-1037.

15. W. P. Mason, Electromechanical Transducers and Wave Filters, 2nd ed.,
     D. Van Nostrand, NY, 1948.

INITIAL DISTRIBUTION LIST

Addressee	No. of Copies
ONR, ONR-220 (A. E. Ellinthorpe), -222	2
NAV SURFACE WEAPONS CENTER, WHITE OAK LAB.	1
NRL, Code 8104 (S. Hanish)	2
NRL, USRD	2
NAVELECSYSCOM, PME-124	1
NAVSEASYSCOM, SEA-63R, -63R12 (C. C. Walker), -63D (Lloyd Epperly), -63X5 (R. E. Heaney), -631Y, -631Y (Surface Sys Sub-Gr)	7
NAVAIRDEVCEN	1
NOSC, Code 7122 (S. Nichols)	2
NOSC, Library, Code 6565	1
NCSC	1
NAVPGSCOL	1
APL/UW, SEATTLE	1
ARL/PENN STATE, STATE COLLEGE	1
DTIC	1
ARL, UNIV OF TEXAS	1
MARINE PHYSICAL LAB, SCRIPPS	1
ONT (Joel Sinsky)	1
AUWE, Portland, Dorset, U.K.	1
DREA, Dartmouth, N.S., Canada	1
NTIS, Arlington, VA	1
General Dynamics, Electric Boat, Dept 443 (J. D. Brown)	1
Design Automation, Inc., 809 Mass. Ave., Lexington, MA 02173	1
Honeywell Marine Systems (D. Hutchins), 5303 Shilshole Ave., N.W. Seattle, WA 98107	1
Sanders Associates (R. White), 95 Canal St., Nashua, NH 03061	1
Raytheon Submarine Signal Div., P.O. Box 360, Portsmouth, RI 02871	1
General Electric, Farrell Road Plant, Syracuse, NY 13201	1
Westinghouse Ocean Research Lab., Box 1488, Annapolis, MD 21404	1
Bendix Electrodynamics Div., 15825 Roxford St., Sylmar, CA 91342	1
International Transducer Corp., 640 McCloskey Place, Goleta, CA 93017	1
Hydroacoustics, Inc., Box 23447, 999 Lehigh Station Rd., Rochester, NY 14892	1